Environ Sci Pollut Res (2014) 21:3197–3217
DOI 10.1007/s11356-013-2313-6

REVIEW ARTICLE

Metal oxide-coated anodes in wastewater treatment

Anantha N. Subba Rao · Venkatesha T. Venkatarangaiah

Received: 2 September 2013 / Accepted: 29 October 2013 / Published online: 29 November 2013

Abstract Electrochemical oxidation is an effective wastewater treatment method. Metal oxide-coated substrates are commonly used as anodes in this process. This article compiles the developments in the fabrication, application, and performance of metal oxide anodes in wastewater treatment. It summarizes the preparative methods and mechanism of oxidation of organics on the metal oxide anodes. The discussion is focused on the application of SnO_2, PbO_2, IrO_2, and RuO_2 metal oxide anodes and their effectiveness in wastewater treatment process.

Keywords Dimensionally stable anodes · Dopant · Incineration · Electrochemical oxidation · Electrocatalytic activity · Dip coating · Sol–gel

Abbreviations

AO7	Azo dye acid orange 7
AOX	Adsorbable organohalogens
ALD	Atomic layer deposition
BDD	Boron-doped diamond
COD	Chemical oxygen demand
DCP	Dichlorophenol
DSA	Dimensionally stable anode
OA	Oxalic acid
OER	Oxygen evolution reaction
PFBA	Perfluorobutanoic acid
PFCA	Perfluorocarboxylic acid
PFDA	Perfluorodecanoic acid
PFHpA	Perfluoroheptanoic acid
PFHxA	Perfluorohexanoic acid
PFPA	Perfluoropentanoic acid
PFNA	Perfluorononanoic acid
PFOA	Perfluorooctanoic acid
RB-4	Reactive Blue 4
RO-16	Reactive Orange 16
SCE	Standard calomel electrode
SEM	Scanning electron microscopy
TOC	Total organic content
XPS	X-ray photoelectron spectroscopy

Responsible editor: Angeles Blanco

A. N. Subba Rao · V. T. Venkatarangaiah (✉)
Department of P.G. Studies and Research in Chemistry,
School of Chemical Sciences, Kuvempu University,
Shankaraghatta 577451, Karnataka, India
e-mail: drtvvenkatesha@yahoo.co.uk

Introduction

Dyes, toxic organic molecules, inorganic salts, adsorbable organohalogens (AOX), aromatic pesticide residues, drugs, and surfactants are the major components of wastewater released from textile, leather, pulp and paper, printing, photograph, cosmetic, pharmaceutical, and food industries (Fornazari et al. 2012; Zaviska et al. 2009). The environmental concern has led to stringent rules and it is mandatory to treat the wastewater before disposing into natural water streams. Chemical, physicochemical, biological/enzymatic, advanced oxidation processes, and electrochemical methods are commonly employed in wastewater treatment (Brungs et al. 1996; Cheng-chun and Jia-fa 2007; Guinea et al. 2009; Hou et al. 2009; Martínez-Huitle and Brillas 2009; Rosales et al. 2009). In the past few years, "electrochemical method" has drawn much attention. It is economical and easy to construct and operate. More importantly, electrodes serve as immobilized active surfaces for the oxidation of organics (Fornazari et al. 2012). In addition, unlike chemical methods, electrochemical method does not necessitate the addition of chemical reagents. However, the addition of electrolyte is inevitable if the wastewater sample is not sufficiently conducting. In many cases, the electrolyte is deliberately added to enhance the degradation process. The added electrolyte strongly influences the efficiency of the process. In exploiting this method as a powerful tool in wastewater treatment, the key part of the electrolytic system—"electrode"—acquires utmost importance.

On oxidation, the organic contaminant undergoes complete oxidation to CO_2 and H_2O (combustion) or results in the

formation of simpler fragments (conversion) (Comninellis 1994). On the other hand, reduction of organics cannot completely lower the chemical oxygen demand (COD) of the wastewater sample, but only leads to poor decontamination (Martínez-Huitle and Brillas 2009). Electrooxidation favors the effective removal of organics over electro-reduction.

Anode is the oxidation site in any electrolytic system. Long service life, large surface area, wide operating potential window between hydrogen and oxygen evolution reaction (OER) overpotentials, high catalytic activity, physically stable, resistant to corrosion, cheap, and easy to fabricate are the prerequisite properties intended to be fulfilled by the anodes employed in electrochemical wastewater treatment.

The anode materials like stainless steel, glassy carbon, Ti/RuO_2, Ti/Pt-Ir, activated carbon fibers, MnO_2, Pt carbon black, porous carbon and reticulated vitreous carbon, and electrodes made of lead, iron, and graphite usually undergo deformation during electrolysis (Martínez-Huitle and Ferro 2006; Rodgers et al. 1999). Beer introduced the titanium substrate-based RuO_2 and TiO_2-coated electrode, referred as dimensionally stable anodes (DSA®s) which possessed high catalytic activity and stability (Beer 1980; Chandler et al. 1997). Figure 1 is the flow chart showing the development of DSA® and DSA®-type metal oxide electrodes (Chandler et al. 1997; Chen et al. 2001, 2002; Klamklang et al. 2012; Nikolić et al. 2012; Panić and Nikolić 2007; Trasatti 2000). The DSAs are good conductors, exhibit high catalytic activity, dimensionally stable, and contribute towards energy savings (see Table 1). They exhibit extended operating life of 8–9 years, without deformation, and their durability has been established in many fields (Chandler et al. 1997; Chen et al. 2002).

The metal oxide electrodes with stability comparable with DSA tempted several research teams to investigate their performance in the electrochemical wastewater treatment. The metal oxide electrodes prepared by Comninellis and Vercesi (RuO_2, IrO_2, TiO_2, ZrO_2, and Ta_2O_5) over Ta substrate exhibited high oxygen evolution overpotential. But, due to high cost of Ta, the other metal Ti was selected as the substrate, and ever since, Ti has been the favorite substrate for the fabrication of metal oxide-coated anodes. Titanium is a cheap "self-healing" substrate which anodically generates a layer of TiO_2 and protects itself against corrosion (Beer 1980). Moreover, the water quality is not affected by the dissolution of Ti in low concentrations (Niu et al. 2012). Ti/tin dioxide (SnO_2), Ti/lead dioxide (PbO_2), and platinum group metal oxide coated on valve metals (Ti, Zr, Ta, Nb, Hf, W) (DSA®s) are the exhaustively studied metal oxide electrodes.

Numerous combinations of these modified metal oxides have been fabricated and tested for their stability, catalytic activity, and ability to incinerate the organics. The ultimate goal is to fabricate an electrode which satisfies the prerequisite properties of the anode. Though few research teams have been successful in fabricating the electrodes with excellent catalytic activity and stability, the search for the best recipe still continues! This review outlines the developments in the preparation, properties, and application of metal oxide-coated anodes in the electrochemical wastewater treatment.

Fabrication of metal oxide anodes

The metal oxide anodes are cheap and easy to fabricate (Gaber et al. 2012; Klamklang et al. 2012; Kusmierek et al. 2011; Yang et al. 2009). Designing and fabricating an electrode of desired composition and characteristics is a challenging task. Thin film metal oxide coatings are prepared by solution phase and gas phase chemical methods. The solution phase method involves dip coating, spin coating, painting, spray pyrolysis, and sol–gel techniques, which employ a precursor solution (Perednis and Gauckler 2005). The gas phase methods are chemical vapor deposition (CVD) and atomic layer deposition (ALD) (Perednis and Gauckler 2005). Electrochemical method (electrochemical anodization and electrochemical deposition) is also widely utilized in the preparation of metal oxide-coated electrode.

A precursor solution is generally prepared by dissolving stoichiometric quantities of metal salts in a solvent or mixture of solvents. The resultant solution is applied on the surface of a substrate using suitable coating techniques [*dip coating* (Watts et al. 2008; Yang et al. 2009), *spin coating* (Fierro and Comninellis 2010), or *painting* (del Río et al. 2009)]. The spin coating technique gives uniform coat on flat substrates. For uneven substrates, dip coating or painting is preferred. The process of coating and drying is repeated until a desired thickness of the coat is obtained. Finally, the coated substrate is annealed to obtain superior morphological characteristics and wear resistance (Comninellis and Vercesi 1991). Thermal decomposition method was adopted in the fabrication of Ti/SnO_2-Sb_2O_3 (Yang et al. 2009), Ti/TiO_2-RuO_2 (Kusmierek et al. 2011; Fachinotti et al. 2007), and Ti/SnO_2-Pt-antimony (Sb) (del Río et al. 2009) electrodes.

Spray pyrolysis is an aerosol process. It is relatively simple and cost effective (Lipp and Pletcher 1997; Perednis and Gauckler 2005; Vicent et al. 1998; Yusta et al. 1997). It involves the atomization of precursor and conversion of these droplets into solid particles by heating. The nature of the deposit obtained on the substrate is dependent on the transformations undergone by the droplets. The temperature gradient between the spraying nozzle and the substrate, the carrier gas and precursor solution flow velocity, and shape and nature of the substrate influence the transformations undergone by the droplets (Correa-Lozano et al. 1996a, 1997). Correa-Lozano et al. (1996a) prepared Ti/SnO_2-Sb_2O_5 electrode using spray pyrolysis technique and have thoroughly studied its characteristics (Correa-Lozano et al. 1996b, 1997).

The *sol–gel* method is also widely used in the fabrication of metal oxide anodes (Attia et al. 2002; Brinker et al. 1991;

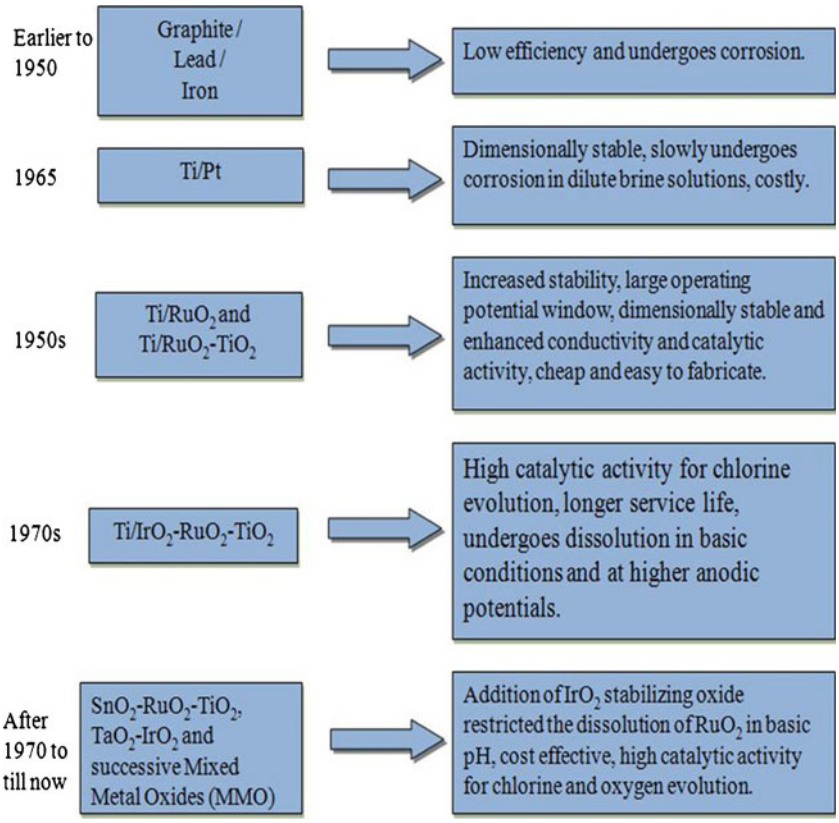

Fig. 1 Flow chart of development of DSA® and DSA®-type metal oxide electrodes

Choi et al. 2007; Panić et al. 2003a, b, 2010; Lu et al. 2010; Ozer et al. 1995). In this method, the microstructure of the coating depends on pH and viscosity (Ozer et al. 1995). Generally, the precursor salts are hydrolyzed by dispersing them in an appropriate media and vigorously stirred for certain ageing time. The formation of solid phase particles of the sol from hydrolyzed precursor is dependent on ageing time. Electrodes prepared at different ageing time differ in their electrochemical behavior (Panić et al. 2003a).

A uniform metal oxide coating of desired thickness can be achieved by *electrochemical* method by adjusting its operating conditions. In electrochemical anodization, a pretreated metal substrate is anodized in a suitable electrolytic bath. A layer of metal oxide coat is generated on the surface of the anodized metal. In electrochemical deposition, precursor salts are dissolved in the electrolytic bath, which are electrodeposited on the substrate. The electrochemical method is advantageous in achieving effective doping and a uniform metal oxide coat on the substrate. Electrochemical method was adopted in the preparation of the following electrodes: Ti/SnO_2-Sb_2O_3-Nb_2O_5/PbO_2 (Yang et al. 2009), Er-chitosan-F-PbO_2 (Wang et al. 2010b), C/PbO_2, Pb + Sn/PbO_2-SnO_2, Pb/PbO_2 (Gaber et al. 2012), Ti/PbO_2 (Panizza and Cerisola 2008), Ti/SnO_2-Sb_2O_5/PbO_2 (Liu and Liu 2008), Pb/PbO_2 (Martínez-Huitle et al. 2008), and Ti/SnO_2-Sb/PbO_2-Ce (Niu et al. 2012).

Table 1 Performance data of different anode materials used in chlor-alkali industry

Anode material	Chlorine overpotential (mV)	Weight loss from anode[a]
Graphite	≈400	2–3 kg/tonne Cl_2
Platinum	≈200	0.4–0.8 g/tonne Cl_2
RuO_2-TiO_2	≈50	<0.03 g/tonne Cl_2

Adapted from the Chandler et al. (1997)

[a] Reaction conditions are as follows: 25 % brine at 363 K; current density, 3 kA m^{-2}

The gas phase techniques are also well known, but they require sophisticated instruments and are relatively costly. In CVD, generally the reactant (precursors) gases are pumped into the reaction chamber maintained at optimum temperature and pressure, where these reactive gases adsorb and react with the substrate to form a thin film. Metal organic chemical vapor deposition utilizes organometallic compounds as precursors (Amjoud et al. 1998; Duverneuil et al. 2002; Devilliers et al. 2003). The ALD technique is closely related to CVD, but the factor which distinguishes it from CVD is that the precursors are led on to the substrate alternately, one at a time (Riihelä et al. 1996). Using CVD, thin films with high uniformity can be reproduced. However, it involves complex processes, high temperature, and toxic gases. Few teams have used gas phase methods for the preparation of thin film metal oxide-coated electrodes (Watts et al. 2008; Yusta et al. 1997; Amjoud et al. 1998; Duverneuil et al. 2002). However, the earlier studies

revealed that in majority of the cases, solution method was preferred for the preparation of metal oxide electrodes. The conditions used in the fabrication of different metal oxide-coated electrodes by solution method are presented in Table 2.

Mechanism of electrochemical oxidation of organics on metal oxide anodes

Figure 2 displays various electrochemical methods used for wastewater treatment. The electroflocculation and electrocoagulation methods produce large amount of sludge, whereas such problem is not encountered in the case of electrooxidation (Mao et al. 2008). The organics in the wastewater are converted into simple molecules and/or completely incinerated to CO_2 and H_2O by electrochemical oxidation (Comninellis 1994). The morphology and composition of the metal oxide coating, nature of the contaminating organic molecule, and wastewater matrix influence the mechanism of oxidation of organics and hence the products (Martínez-Huitle and Ferro 2006).

Mechanism of oxidation

Oxidation of organics proceeds as follows:

- By direct electron exchange with the anode (direct oxidation)
- By the active species during electrolysis (indirect oxidation)

The direct exchange of electrons between the anode material and the organic molecule at the electrode solution interface is referred as "direct oxidation." This reaction is viable at potentials well below the oxygen evolution overpotential. But the anode surface gradually undergoes passivation due to adsorption of organic molecules (Panizza and Cerisola 2009).

A theoretical model for the mechanism of oxidation of organics on metal oxide anodes was proposed by Comninellis (1994), and it has been accepted by the scientific community. During electrolysis, hydroxyl ($^{\bullet}OH$) radicals are generated on the anode surface by water discharge at high anodic potentials (Panizza and Cerisola 2009; Watts et al. 2008). These $^{\bullet}OH$ radicals adsorb physically (Eq. 1) or chemically (Eq. 2) on the metal oxide anode (MO_x).

$$MO_x + H_2O \rightarrow MO_x(\cdot OH) + H^+ + e^- \quad (1)$$

$$MO_x(^{\bullet}OH) \rightarrow MO_{x+1} + H^+ + e^- \quad (2)$$

As a result of strong interaction between hydroxyl radical ($^{\bullet}OH$) with the anode metal and availability of a higher oxidation state for the anode metal leads to the formation of MO_{x+1} (Martínez-Huitle and Ferro 2006).

Table 2 Fabrication of metal oxide-coated anodes

Electrode	Precursors	Solvent and coating technique	Annealing temperature (°C)	Reference
Ti/SnO_2-Sb_2O_3	$SnCl_4{\cdot}5H_2O + Sb_2O_3$	Isopropanol + conc. HCl, dip coating	480	Yang et al. (2009)
Al/Sb_2O_5	$SbCl_3$ (1.753 g)	Isopropanol + conc. HCl (10:0.5), painting	550	Soni and Ruparelia (2012)
Fe/SnO_2-Sb_2O_5	$SnCl_4\ 5H_2O + SbCl_3$ (1.227 g + 0.342 g)	Isopropanol + conc. HCl (10: 0.5), painting	550	
Ti/SnO_2-Sb	$SnCl_4\ 5H_2O + SbCl_3$ Sb/(Sn + Sb)=2.9 to 20 %	Isopropanol + conc. HCl, painting	450	Mao et al. (2008)
$Ti/SnO_2 + Sb_2O_5$	$SnCl_4\ 5H_2O + SbCl_3$ $SnCl_4{\cdot}5H_2O/SbCl_3$=20:1 %	Isopropanol + conc. HCl, dip coating	500	Watts et al. (2008)
$Ti/SnO_2 + Sb_2O_5$	$SnCl_4{\cdot}5H_2O + SbCl_3$	92 % isopropanol + 8 % HCl, dip coating	500	Jiang-tao et al. (2007)
Ti/SnO_2-Pt-Sb	$SnCl_4{\cdot}5H_2O + SbCl_3 + 2PtCl_6\ 6H_2O$ Sn/Sb/Pt=10:1:0.252	Ethanol + conc. HCl, painting	600	del Río et al. (2009)
Ti/SnO_2-Sb	$SnCl_4{\cdot}5H_2O + SbCl_3$	Ethanol, painting	550	Costa et al. (2010)
Ti/SnO_2-Sb-Ir	$SnCl_4{\cdot}5H_2O + SbCl_3 + IrCl_3{\cdot}xH_2O$ Sn/Ir=9:1	Ethanol, painting	550	
Ti/SnO_2-Sb_2O_3	$SnCl_4{\cdot}5H_2O + SbCl_3$ (8.5+5 g)	*n*-Butanol + HCl (40+10 mL), painting	500	Wang et al. (2010a)
Ti/SnO_2-Sb-La	$SnCl_4{\cdot}5H_2O + SbCl_3$ Sn/Sb/La=100/6/2	Citric acid (CA) + ethylene glycol (5 mL) + ethanol (30 mL). Molar ratio of metal/CA/ ethylene glycol=1:3:3, painting	550	Xu et al. (2012)
Ti/SnO_2-Sb-Ru	$SnCl_4{\cdot}5H_2O + SbCl_3$ Sn/Sb/Ru=100/6/2		550	
Ti/SnO_2-Sb	$SnCl_4{\cdot}5H_2O + SbCl_3$ Sn/Sb=100/6		550	

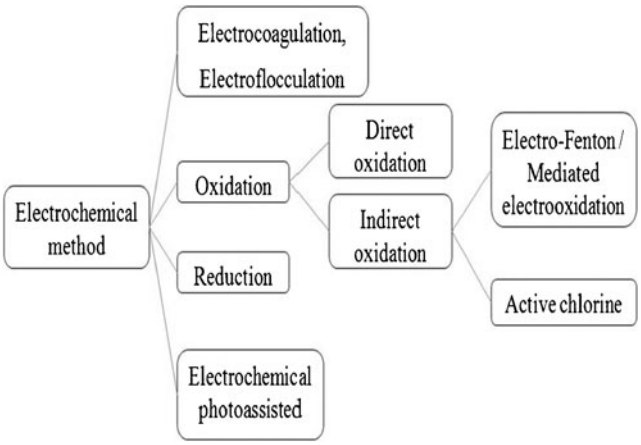

Fig. 2 Electrochemical methods. Adapted from Martínez-Huitle and Brillas (2009)

Electrodes which can undergo such interaction are referred as "active" (carbon, graphite, IrO_2, RuO_2, platinum) (Panizza and Cerisola 2009). "Non-active" anodes (SnO_2, PbO_2, or boron-doped diamond (BDD)) only act as inert electron sink for the removal of electrons from organics, without providing any adsorptive site (Comninellis 1994; Ozer et al. 1995). Chemisorbed oxygen in MO_{x+1}/MO_x couple acts as an active site for the selective oxidation of organics (Eq. 5), whereas physisorbed $^{\bullet}OH$ radicals completely incinerate the organics into CO_2 and H_2O (Eqs. 3 and 4) (Comninellis 1994).

$$MO_x(^{\bullet}OH) + RH \rightarrow MO_x + H_2O + R^{\bullet} \quad (3)$$

$$MO_x(^{\bullet}OH) + R^{\bullet} \rightarrow MO_x + CO_2 + H_2O \quad (4)$$

$$MO_{x+1} + R \rightarrow MO_x + \text{Intermediates} \quad (5)$$

The oxygen evolution reaction (Eqs. 6 and 7) always competes with the oxidation reaction of organics.

$$MO_x(^{\bullet}OH) \rightarrow MO_x + {}^1/_2\ O_2 + H^+ + e^- \quad (6)$$

$$MO_{x+1} \rightarrow MO_x + {}^1/_2\ O_2 \quad (7)$$

Figure 3 is the schematic diagram of electrochemical oxidation of organics on metal oxide anodes.

Oxidation by electrochemically generated oxidants

On electrolysis, species generated by the discharge of water (hydroxyl radical, hydrogen peroxide, ozone) react with themselves or with the electrolytes to produce active oxidants. These oxidants are utilized in the oxidation of organics and this type of oxidation is referred as "indirect oxidation" (Jüttner et al. 2000; Li et al. 2009; Martínez-Huitle and Ferro 2006; Panizza et al. 2000; Scialdone 2009; Scialdone et al. 2009b; Simond et al. 1997b; Zhao et al. 2003). Mediated electrooxidation involves metal ions with high oxidation potential. In this method, oxidants are electrochemically generated in a closed cycle and can completely incinerate the organics (Jüttner et al. 2000).

Different electrolytes could be found in any industrial effluent. Chloride salts are most common. It is observed that the presence of chloride (Cl^-) ions in the wastewater increases the organic removal efficiency (Comninellis 1994; Scialdone et al. 2009b). Electrochemically generated active chlorine species efficiently oxidize the organics as per Eqs. 8–11 (Jüttner et al. 2000; Martínez-Huitle and Ferro 2006; Panizza et al. 2000; Scialdone et al. 2009b).

$$2Cl^- \rightarrow Cl_{2(aq)} + 2e^- \quad (E^o = 1.40\,V \text{ vs. SHE}) \quad (8)$$

$$Cl_{2(aq)} + H_2O \rightarrow HOCl + H^+ + Cl^- \quad (E^o = 1.49\,V \text{ vs. SHE}) \quad (9)$$

$$HOCl \leftrightarrow H^+ + OCl^- \quad (E^o = 0.89\,V \text{ vs.SHE}) \quad (10)$$

$$R + OCl^- \rightarrow \text{Intermediates} \rightarrow CO_2 + H_2O + Cl^- \quad (11)$$

The equilibrium in Eq. 10 is pH dependent. HOCl predominates in the pH range 3–8 and ClO^- predominates above pH 8 (Fornazari et al. 2012; Malpass et al. 2012). Hence, oxidation of organics by HOCl is favorable at near neutral pH (Fornazari et al. 2012; Malpass et al. 2012). The Cl_2/Cl^- and $HOCl/Cl_2$ couples also oxidize the organics completely (Fornazari et al. 2012; Song et al. 2010b). The electrochemical reactions at the anode surface involving chloride ions are given in Eqs. 12 and 13 (Scialdone et al. 2009b):

$$MO_x(\cdot OH) + Cl^- \rightarrow MO_x(HOCl) + e^- \quad (12)$$

$$MO_x(HOCl) + R \rightarrow \text{Intermediates} \rightarrow MO_x + CO_2 + H_2O + Cl^- + H^+ \quad (13)$$

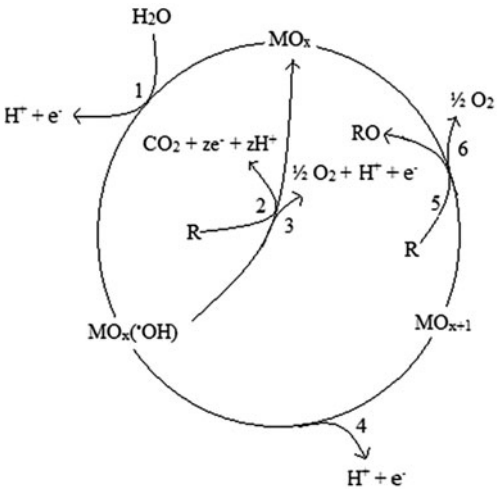

Fig. 3 Electrochemical oxidation of organics on metal oxide MO_x anode. *1* Water discharge. *2* Combustion of R (organic molecule). *3* and *6* O_2 evolution. *4* Higher oxide formation. *5* conversion of R to RO. Adapted from Comninellis (1994) and Simond et al. (1997a).

MO_x(HOCl) mediates unselective oxidation and thereby provides substantial total organic carbon (TOC) removal (Fornazari et al. 2012). However, the presence of chloride ions is associated with the following disadvantages: the formation of AOX (Malpass et al. 2012; Sakalis et al. 2007) and the generation of ClO^-. AOXs are toxic and recalcitrant to degradation, and ClO^- reduces the service life of the metal oxide anode (Costa et al. 2010). Several other electrolytes like ClO_4^-, NO_3^-, PO_4^{2-}, SO_4^{2-}, CO_3^{2-}, and Br^- were tested for electrochemical degradation process (Fornazari et al. 2012; Gaber et al. 2012). But the degradation efficiency in presence of Cl^- ions was found to be better than that achieved in the presence of these electrolytes. The peroxidisulfate is a powerful oxidizing agent and as effective as hydroxyl radical (Malpass et al. 2012). Excellent degradation of organics is possible in presence of sulfate ions, provided that the electrode and the wastewater environment matrix favors the formation of sulfate radical or peroxidisulfate ion (Martínez-Huitle et al. 2008; Martínez-Huitle et al. 2008; Brillas et al. 2009). However, the COD/TOC removal not only depends on the electrode and electrolytes, but also on the organic molecule itself (Marugán et al. 2007).

Factors influencing the anode performance

The performance of an electrode is rated in terms of its ability to incinerate the organics with minimum consumption of energy and time. The nature of the electrode, applied current density, duration of electrolysis, supporting electrolyte, pH, temperature, and cell geometry significantly contribute to the efficiency and energy consumption of the electrochemical oxidation process. The nature of the electrode is dependent on its fabrication technique, composition, and structure.

Fabrication technique

Both physical (surface morphology, metal oxide film thickness, composition, dimension, microstructure) (Wang et al. 2009) and chemical (availability of higher oxidation state, its affinity towards hydroxyl radicals, stability in different pH, active species generated in presence of different electrolytes, and wear-tear) properties of an anode influence its ability to oxidize the organics (electrochemical activity) or to generate active oxidants (electrocatalytic activity). The fabrication technique can modulate both the chemical and physical nature of the coating and hence its electrocatalytic and electrochemical activities.

Proper substrate pretreatment is the key to produce a strong adhesion of metal oxide coating on the surface of the substrate (Beer 1980). The solvents used in the precursor solution, dopant and its content, coating technique, dip withdrawal rate, and annealing temperature are crucial factors which contribute in altering the characteristics of an anode. The schematic representation of the steps involved in the fabrication of metal oxide anodes by thermal decomposition is shown Fig. 4 (Comninellis and Guohua 2010).

The solvents used in the preparation of precursor solution play a role of great consequence in altering the morphology and hence the characteristics associated with the morphology (exposure of catalytic and adsorptive sites, porosity, and effective surface area) of the metal oxide coating. The difference in the thermal expansion coefficient of the base metal and the coating leads to the formation of cracks in the coating and results in typical cracked mud coating (Jiang-tao et al. 2007; Wang et al. 2009). Cracked mud coating gradually undergoes erosion. The adsorption capacity is favored by the irregular electrode surface. But it involves undesired strong adsorption of hydroxyl radicals as well. Weak interaction between the electrode surface and hydroxyl radicals increases electrochemical activity of the electrode towards the oxidation of organics, whereas strong interaction results in oxygen evolution (Costa et al. 2010; Kapałka et al. 2008). The efficiency of the process decreases with oxygen evolution.

Three different precursor solutions prepared in ethanol, *n*-butanol and a polymeric precursor were used in the fabrication of SnO_2 + Sb_2O_3 interlayer by thermal decomposition (Wang et al. 2009). The scanning electron microscopy (SEM) images in Fig. 5 clearly reveal the morphological differences in the oxide interlayer obtained from these precursor solutions. The oxide interlayer from the polymeric precursor assisted the structural alignment and produced more agglomerated coating, whereas alcoholic precursors produced typical cracked mud coating.

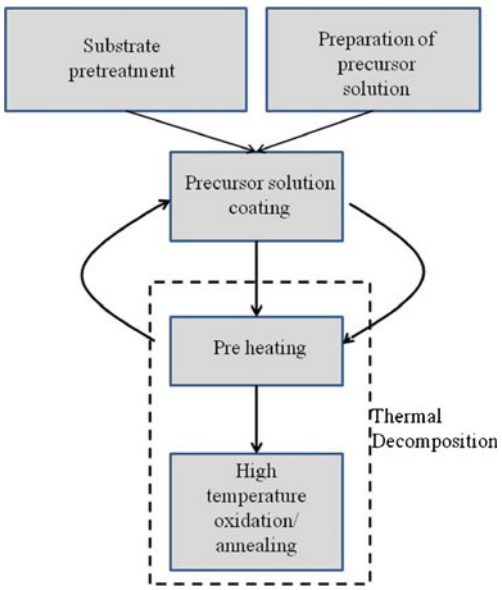

Fig. 4 Schematic diagram of steps involved in the fabrication of metal oxide electrodes by thermal decomposition technique. Adapted from Comninellis and Guohua (2010)

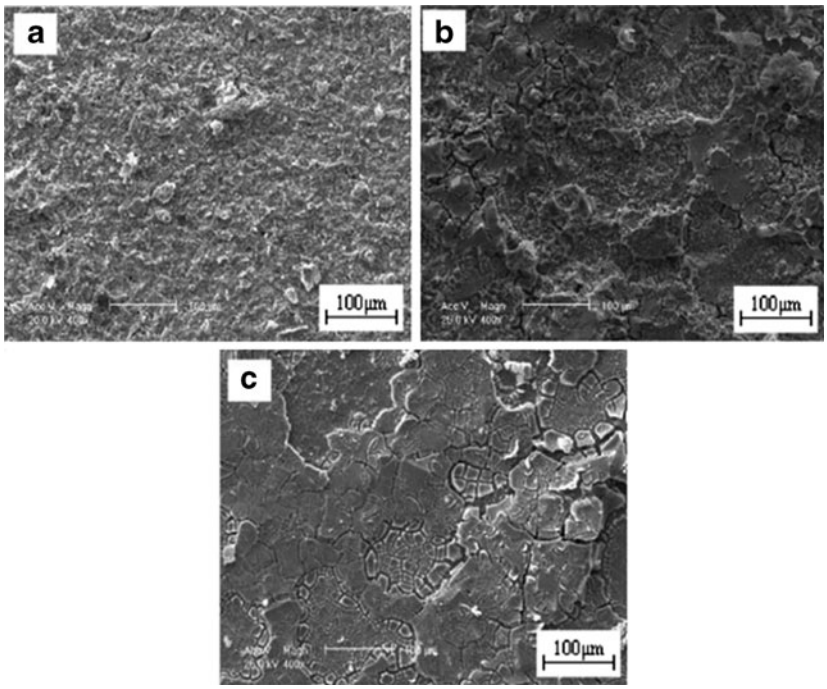

Fig. 5 SEM micrographics of SnO_2 + Sb_2O_3 coatings prepared with different precursor solvents: **a** polymeric precursor, **b** ethanol, and **c** *n*-butanol. Reprinted from Wang et al. (2009). Copyright 2008 Elsevier

The nature of the precursor solution can significantly affect the host metal and dopant content in the coating. It was found that viscous precursor solutions aid in the formation of agglomerated uniform coating and accumulation of the dopant on the surface of the coating, whereas alcoholic precursor solutions lead to cracked mud coating. Precursor solution prepared in isopropanol and sol–gel was used in the fabrication of Sb-SnO_2/Ti electrode by thermal decomposition. The Sn/Sb content in the coating was found to be higher than in the alcoholic precursor solution (Wang et al. 2010a; He and Mho 2004). On the contrary, the Sb content was found to be higher in the coating than in the solution when sol–gel method was adopted (Wang et al. 2006).

Antimony is the most commonly used dopant in the preparation of SnO_2 electrodes and it is the hydroxyl radical generation site (Jiang-tao et al. 2007). Hence, its accumulation on the surface of the coating is recommended. Variation in the Sb content considerably influences the morphology of the coating.

The electrocatalytic activity can be enhanced by minimizing the interlayer thickness and maximizing the outer active surface area by choosing the right combination of techniques in the preparation of metal oxide electrodes (Yeo et al. 2010). Different preparative methods were used in combination by Yeo et al. (2010) to obtain a compact layer of metal oxide coat. They prepared Ti/Pb(E)/PbO_2(T,E) (E-electrodeposition, T-thermal decomposition) electrode by electrodepositing a layer of Pb on Ti, followed by coating a layer of PbO by thermal decomposition. The PbO was then electrooxidized to PbO_2. This electrode acquired large surface area and roughness. The relative roughness factor of this electrode was found to be 8.98, where the arbitrary roughness factor of Ti/Pb(E)/PbO_2 (E) electrode was set as unity. Watts et al. (2008) found that the dopant content, coating technique, and the annealing temperature are the major factors which contribute significantly in controlling the characteristics of a metal oxide coat. The effect of number of layers of the coating and dip withdrawal rate on the performance of the electrode in eliminating the organics was found to be very feeble.

Interfacial layer or undercoat

The oxygen which evolved at the anode surface creeps through the metal oxide coating and passivates the substrate metal. This is eliminated by the inclusion of an interfacial layer connecting the active metal oxide coating and the substrate. The chemical stability, resistance against corrosion, and service life of the anode are enhanced by the insertion of an interlayer (Kong et al. 2012). An undercoat of stable metal oxide is applied on a substrate and then an outer active layer is overlaid. It is represented as substrate/interlayer/active surface layer as shown in Fig. 6. The interlayer supports the active metal oxide layer to adhere strongly onto the substrate and helps in guarding the stability and enhancing the electrocatalytic activity of the electrode. It is important for the interlayer to be highly conducting and itself does not undergo passivation. The constituent metals of the interlayer should satisfy

Fig. 6 Representation of multilayer metal oxide-coated substrate

the Hume-Rothery limit (15 %) between their ionic radii, so that a solid solution between the three layers is possible.

The direct deposition of PbO_2 on Ti substrate by electrodeposition leads to the formation of a passive layer of TiO_2 (Yang et al. 2009). This can be avoided by depositing an interlayer on Ti substrate. The interlayer acts as a barrier against such passivation of the substrate by avoiding the diffusion of oxygen. For the interlayer in Ti/solid solution interlayer/PbO_2 electrode, the metals chosen by Kong et al. (2012 were such that the ratios of their corresponding ionic radii (Sn/Sb, Ru/Ti, Ir/Ta) were below the Hume-Rothery limit. Figure 7 is the SEM images of the interlayer surfaces SnO_2-Sb_2O_5, RuO_2-TiO_2, and IrO_2-Ta_2O_5 (Kong et al. 2012). The ionic radii ratio of the metals in the interlayer to Ti^{4+} obtained from the oxidation of Ti substrate also lays within the limit; hence, excellent binding was obtained between the interlayer and the substrate. Similarly, the interlayer and the electrodeposited PbO_2-active layer formed a continuous solid solution, except in the case of RuO_2-TiO_2 interlayer, which provided only partial solid solution with the PbO_2 due to large difference in the ionic radii of Ti^{4+} and Pb^{4+}. The interlayer enhanced the orientation of the crystal structure of the electrodeposited PbO_2. Ti/IrO_2-Ta_2O_5/PbO_2 electrode coating showed high catalytic activity for oxygen evolution. The inclusion of IrO_2-Ta_2O_5 interlayer in Ti/PbO_2 electrode increased its service life from 11 to 672 h as determined by the accelerated lifetime test in 1 M H_2SO_4 under galvanostatic condition (4 A cm^{-2}). RuO_2-TiO_2 and SnO_2-Sb_2O_5 interlayers showed intermediate enhancement in service life of 207 and 58 h, respectively. The interlayer effectively eliminated the passivation of Ti substrate and enhanced the performance of the anode towards oxidation of organics. Similar results were obtained from the electrodes with interlayers of different composition (see Tables 2, 3, and 4).

Metal oxides in wastewater treatment

Several mixed metal oxide electrodes have been used in the electrochemical wastewater treatment. Nevertheless, it is found from the literature that majority of these are the derivatives of four metal oxides, SnO_2, PbO_2, RuO_2, and IrO_2, and hence we limit our discussion to these metal oxide electrodes.

SnO_2

Tin oxide is an insulator in its stoichiometric form. The distortions created by the oxygen vacancies make it an n-type and conductive material. Doped SnO_2 anodes (non-active) show excellent conductivity, high oxygen and chlorine evolution overpotential, electrocatalytic activity for the oxidation of organic compounds, ability to adhere strongly to the base metal, and stability over a large pH range (Correa-Lozano et al. 1997; del Río et al. 2009; Jiang-tao et al. 2007;

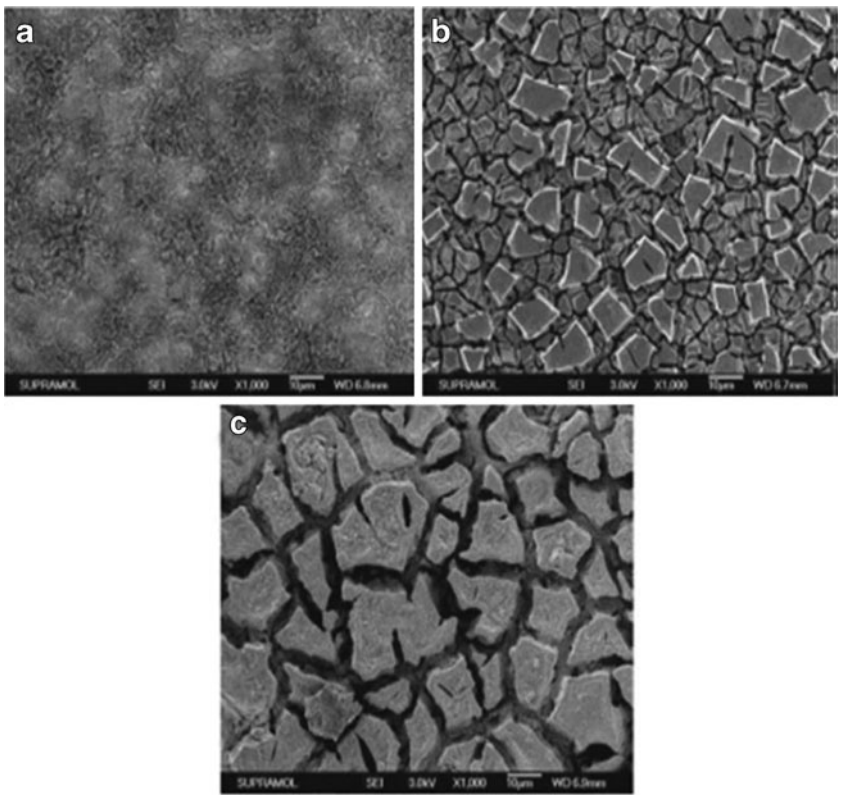

Fig. 7 SEM images of the interlayer surface. **a** Ti/SnO_2-Sb_2O_5. **b** Ti/RuO_2-TiO_2. **c** Ti/IrO_2–Ta_2O_5. Reprinted from Kong et al. (2012). Copyright 2012 Springer Science + Business Media B.V.

Table 3 Performance of different modified SnO_2 anodes and working conditions

Pollutant	Electrode, ASL, ACS	Operating conditions	% COD, TOC removal, %CE, TEC	Remarks	Reference
Synthetic tannery wastewater	1. Ti/SnO_2-Sb	SE=0.1 mol L^{-1} Na_2SO_4, 4 h, j=25	TOC=56.100 %CE=65.000 TEC=0.104	%CE decreased with time Complete electrode Deactivation reached after 4 h	Costa et al. (2010)
	1. Ti/SnO_2-Sb-Ir	SE=0.1 mol L^{-1} Na_2SO_4, 4 h, j=25	TOC=2.100 %CE=2.000 TEC=2.547	Ir doping made no enhancement in TOC removal, but stability of the electrode increased	
Phenol	1. Ti/SnO_2-Sb ASL=28.5 ACS=12.0	IC, 500 mg L^{-1} (100 mL) SE=0.1 M Na_2SO_4, 2.5 h, j=30	COD=60.200 %CE=28.290	ASL test conditions: 1 M H_2SO_4, 40 °C, stainless steel cathode, j=2 A cm^{-2}. Doping with Ru and La substantially increased the service life, crystallite size, conductivity, and surface charge density of Ti/SnO_2-Sb	Xu et al. (2012)
	2. Ti/SnO2-Sb-Ru ASL=34.0 ACS=9.7		COD=82.100 %CE=38.630		
	3. Ti/SnO2-Sb-La ASL=35.5 ACS=8.6		COD=86.400 %CE=40.650		
Methamidophos (*O*,*S*-dimethyl phosphoramidothioate) (MMD)	1. Ti/SnO2	IC=50 mg L^{-1} (100 mL), SE: Na_2SO_4, j=10, 20, 30; pH=2	–	Electrooxidation at all applied current densities was slow	Martínez-Huitle et al. (2008)
PFOA	1. Ti/SnO2-Sb-Bi ASL=0.8 h	IC=100 mg L^{-1} (200 mL), 2 h; SE, 1.4 g L^{-1}	PFOA removal ratio=89.8	ASL conditions: j=100 mA cm^{-2}, 0.5 M H_2SO_4 until cell potential reached 5 V from initial value	Zhuo et al. (2011)
	2. Ti/SnO2-Sb ASL=0.4 h		PFOA removal ratio=93.3		

IC initial concentration of the pollutant, *SE* supporting electrolyte, *j* current density (in milliamperes per square centimeter), *%CE* percentage current efficiency, *TEC* total energy consumed (in kilowatt-hours per cubic meter), *ASL* accelerated service life in hours, *ACS* average crystallite size (in nanometers)

Table 4 Performance of different modified PbO_2 anodes and working conditions

Pollutant	Electrode	Operating conditions	% COD and TOC removal, %CE, TEC	Remarks	Reference
	Ti/PbO_2			OER=1.8–2.0 V	Kapałka et al. (2008)
Phenol	1. Ti/SnO_2-Sb_2O_3-Nb_2O_5/PbO_2 AGS 6 μm	IC=0.5 g L^{-1} (50 mL); SE=Na_2SO_4 (7.5 g L^{-1})	COD=78.6	OER= 1.8 V (vs SCE), condition=7.4 g L^{-1} Na_2SO_4, pH 7. No metal dissolution occurred	Yang et al. (2009)
		120 min, j=20, SE: NaCl (21.3 g L^{-1})	COD=97.2	The addition of chloride ions evidently enhanced the COD removal due to the generation of active chlorine species	
Phenol	1. Ti/SnO_2 + Sb_2O_3/PbO_2 ASL=29.5	IC=200 mg L^{-1} (80 mL), 3 h SE, Na_2SO_4, j=15	COD=59.3, instantaneous %CE=45	ASL test conditions: 1 M H_2SO_4, 60 °C, Cu cathode, j=4 A cm^{-2}, until cell potential reached 5 V from initial value. Electrochemical activity for the oxidation of phenol is in the order 1 > 2 > 3. The solvent used in the preparation of precursor solution affected the service life of the electrodes	Wang et al. (2009)
	2. Ti/SnO_2 + Sb_2O_3/MnO_x ASL=39.2		COD=45.7, instantaneous %CE<20		
	3. Ti/SnO_2 + Sb_2O_3/RuO_2 + PbO_2 ASL=8.4		COD=37.9, instantaneous %CE<20		
Real wastewater sample containing Reactive Yellow 160	1. Pb + Sn/PbO_2 + SnO_2	IC=100 mg L^{-1}, SE: NaCl (4 g L^{-1}), pH=7.13, j=50 380 min	COD=100	The effect of NaCl, KCl, $CaCl_2$, Na_2CO_3, NaF, Na_3PO_4, and Na_2SO_4 supporting electrolytes was investigated. Best results were obtained in presence of chloride ions	Gaber et al. (2012)
	2. C/PbO_2	300 min			
	3. Pb/PbO_2	400 min			
Alphazurine dye	1. Pb/PbO_2	IC=500 mg L^{-1}, SE: Na_2SO_4; j=30 and 60	COD=90, %CE=24, TEC=124	Consumed high energy for the complete incineration of the dye. OER=1.8 V (vs SCE)	Nava et al. (2008)
2,4-Dichlrophenol (2,4-DCP)	1. Ti/SnO_2-Sb_2O_3/F-PbO_2 AGS=5 μm	180 mL, 20 °C 2 h, j=10	COD=71	All 3 electrodes showed good stability against deterioration and passivation. Er doping reduced the grain size and enhanced the degradation and mineralization of 2,4-DCP in the order 3 > 2 > 1	Wang et al. (2010b)
	2. Ti/SnO_2-Sb_2O_3/Er-F-PbO_2		COD=88, TOC=44		
	3. Ti/SnO_2-Sb_2O_3/Er-chitosan-F-PbO_2		COD=95, TOC=53		
Methyl Red	1. Ti/PbO_2	IC=100 mg L^{-1}; current=0.5; FR=240 L h^{-1} (varied from 100 to 240 L h^{-1})	COD=90, %CE-decreased with increasing j. TEC=48	Mineralization rate increased with the flow rate. Performance of PbO_2 was compared with BDD. PbO_2 consumed same energy as BDD, but the rate of mineralization was slow	Panizza and Cerisola (2008)
o-Nitrophenol (k-pseudo-first-order rate constant for the oxidation of *o*-nitrophenol)	1. Ti/β-PbO_2 ACS- 27.929	IC=50 mg L^{-1} (300 mL), SE: Na_2SO_4 + NaCl, j=30	COD=77.8, %CE= 28.14	OER determined in 0.5 M H_2SO_4 solution. 1. OER=1.6 V (vs SCE), k=0.0738/min; 2. OER=1.75 V (vs SCE), k=0.0988/min, highest electrocatalytic activity, porous, compact, and smallest crystallite size. 3. OER 1.55 V (vs SCE),	Liu and Liu (2008)
	2. Ti/Bi–PbO_2 ACS- 17.491		COD=87, %CE=31.49		
	3. Ti/Co–PbO_2 ACS- 27.057		COD=75.9, %CE= 27.47		

Table 4 (continued)

Pollutant	Electrode	Operating conditions	% COD and TOC removal, %CE, TEC	Remarks	Reference
	1. Ti/Bi–Co–PbO_2 ACS- 19.467		COD=83.3, %CE= 30.15	k=0.0716/min. crystalline size decreased on doping. 4. OER 1.70 V (vs SCE), k=0.0411/min. Bi is more effective as dopant than Co. It increased the stability of undoped PbO_2 anode	
Methamidophos (*O*,*S*-dimethyl phosphoramidothioate) (MMD)	1. Pb/PbO_2	IC=50 mg L^{-1} (100 mL), SE: Na_2SO_4, j=30	TOC=85 %	Eighty-five percent mineralization was achieved under j=10 and 20 mA cm^{-2}. COD removal efficiency reached maximum at j k=30, pH=2	Martínez-Huitle et al. (2008)
Reactive Orange 16	1. Ti-Pt/β-PbO_2	IC=85 mg L^{-1} in 0.1 M Na_2SO_4, FR=7 L min^{-1}, SE=50 mM NaCl, j=50		NaCl addition improved the performance by 90 %; 85 % mineralization was achieved with 2.0 A h L^{-1} charge supply. CE=16.7 % with 1.0 A h L^{-1} charge supply	Andrade et al. (2009)
4-Chloro-3-methylphenol (CMP)	1. Ti/SnO_2–Sb/PbO_2 ASL- 175	IC=0.70 mM (80 mL); SE=0.25 M Na_2SO_4, j=10	49 (TOC) instantaneous %CE-initial=20 (for 1 h)	ASL conditions: j=1.2 A cm^{-2}, 9 M H_2SO_4, 90 °C until cell potential reached 5 V from initial value. Addition of NaCl significantly increased the CMP removal. %CE decreased with time	Song et al. (2010a)
Car wash wastewater	1. Ti/PbO_2	FR=300 L h^{-1} 10 h, j=10	COD=97 (at 25 °C), COD=99 (at 40 °C), j=3, A TEC=770	Temperature variation made small influence on COD removal. Small increase in COD removal with flow rate. TEC for BDD=375 kWh m^{-3}	Panizza and Cerisola (2010)
Methyl green	1. Ti/PbO_2	IC=300 mg L^{-1} 0.5 M H_2SO_4; j=10–40	TOC=40 (25 °C), 60 (40 °C), 82 (60 °C); PCE=70, TEC=0.289 (j=10) 1.637 (j=40)	Color removal rate increased with temperature and applied current density	Carvalho et al. (2011)
Sulfamethoxazole (SMX)	1. Ti/SnO_2-Sb/Ce-PbO_2	IC=100 mg L^{-1}, pH 3, distance between electrodes=3 mm, j=5–10	99 % SMX removal	Time required was 32.9–23.0 min, and energy consumed was 26.3–46.3 Wh L^{-1}	Lin et al. (2013b)
PFBA	1. Ti/SnO_2-Sb/PbO_2-Ce	IC=100 mg L^{-1}; SE=10 mM L^{-1} $NaClO_4$ 90 min, j=20	TOC=15.6±1.8	The dissolution of Pb was well within the drinking water ordinance limit. Complete mineralization of PFCA claimed to be possible on this electrode	Niu et al. (2012)
PFPeA			TOC=29.1±2.3		
PFHxA			TOC=65.9±3.1		
PFHpA			TOC=89.4±3.8		
PFOA			TOC=91.7±3.6		

IC initial concentration of the pollutant, *SE* supporting electrolyte, *j* current density (in milliamperes per square centimeter), *FR* electrolyte flow rate in case of recirculation batch systems, **PCE* percentage current efficiency, *TEC* total energy consumed (in kilowatt-hours per cubic meter), *AGS* average grain size (in nanometer), *ACS* average crystallite size, *PFHxA* perfluorohexanoic acid, *PFHpA* perfluoroheptanoic acid

Lipp and Pletcher 1997; Vicent et al. 1998; Xu et al. 2012; Yusta et al. 1997). The deviation in the native defects, nature, and effect of doping into the crystal lattice influences the activity of SnO_2. The oxygen vacant sites are responsible for the conductivity of SnO_2 and also the availability of these vacant sites determines the ratio of MO_{x+1} and MO($^{\bullet}$OH) on the anode surface. If the crystal defect increases with the formation of more of oxygen vacant sites, the formation of MO_{x+1} is favored. The physically adsorbed hydroxyl radical reacts chemically to fill the vacant sites of the crystal lattice to form MO_{x+1}. MO_{x+1} favors only the conversion of organics into oxidized intermediates, whereas MO($^{\bullet}$OH) completely incinerates the organics into CO_2 and H_2O (Feng et al. 2008). The electrocatalytic activity of Ti/SnO_2 electrode is higher than that of PbO_2 and RuO_2/IrO_2 electrodes (Radjenovic et al. 2011; Mao et al. 2008). Moreover, it is comparatively cheaper than the noble metal oxide electrodes and easy to fabricate (Mao et al. 2008).

The empty electron orbitals available on the *f*-block elements can be used as channels for electron transaction from the substrates, if doped into metal oxide coating (Fenga and Li 2003). Electrocatalytic activity of the electrodes for the oxidation of organics markedly improves on doping (Fenga and Li 2003). The dopant and its molar ratio with the host metal oxide influence the physicochemical properties of the electrode. Among the various dopants (B, Bi, Ce, F, Fe, Gd, Ir, La, Ni, Pt, Ru, and Sb) used to enhance the characteristics of the SnO_2, Sb has shown remarkable impact (Jiang-tao et al. 2007; Costa et al. 2010). Sn and Sb ionic radii satisfy the Hume-Rothery limit, and hence, a homogeneous solid solution between the two metals is possible. A list of modified SnO_2 electrodes and conditions used in their fabrication is given in Table 2.

The content of the dopant has a critical role to play in directing the microcrystalline structure, morphology, electrocatalytic activity, and capability of generation of hydroxyl radicals and hence the oxidation of organics. Ti/SnO_2-Sb electrode possesses high OER potential which varies with the composition of Sn/Sb ratio. For the electrodes prepared with varying concentrations of Sb, OER showed potential greater than 1.9 V (vs standard calomel electrode (SCE)) in all the cases and it increased with an increase in Sb content (Mao et al. 2008). The highest catalytic activity was found with 8 mol % [SnO_2-Sb(0.08)] and generated high concentration of oxidants.

The competition between the oxidation reaction and the OER resulted in low efficiency of $Ru_{0.7}Ir_{0.3}O_2$ anode to degrade β-blocker metoprolol and led to the persistence of halogenated derivatives, whereas on SnO_2-Sb electrode, the production of hydroxyl radical was sufficient enough to degrade the metoprolol into simpler intermediates (Radjenovic et al. 2011).

Jiang-tao et al. (2007) doped SnO_2 with 5, 10, and 15 % of Sb and used these electrodes in the electrooxidation of 4-chlorophenol. The oxygen evolution potential for Ti/Sb-SnO_2 with 5 % Sb electrode skipped from 1.5 V (without Sb) to 1.65 V. The oxidizable species in this potential window are oxidized directly on the anode surface. COD removal (48.9 %) of 4-chlorophenol with 15 % current efficiency was obtained on 5 % Sb-doped electrode, whereas for 0, 10, and 15 %, Sb dopant the COD removal was 36.4, 44.8, and 26.6 %, respectively. However, it has also been reported in both cases (Mao et al. 2008; Jiang-tao et al. 2007) that effective and homogeneous distribution of Sb diminished with an increase in Sb content. This was attributed to the difference in the thermal expansion coefficients. This effect is not so strong at lower Sb contents, but at higher content of Sb, the variation in the surface morphology is clearly noticeable. On using high content of dopant, the electrode follows conversion mechanism, due to selective oxidation by the chemisorbed oxygen, as discussed earlier (Kong et al. 2012). At low content of dopant (Sb centers are sites for hydroxyl radical generation), physisorbed hydroxyl radicals are involved in the oxidation leading to complete combustion of the organics. The inhomogeneous distribution of Sb reduces the catalytic activity, and the base metal gets exposed to the electrolytic bath solution leading to its passivation. The dopant not only influences the morphology of the oxide coating, but also controls the mechanism of oxidation of organics on the anode surface. Hence, it is important to choose the right dopant and monitor its content very carefully during the fabrication of an electrode.

Gd (2 mol %)-doped SnO_2-Sb possesses low oxygen vacancies in the crystal lattice of SnO_2 than undoped SnO_2-Sb (Feng et al. 2008). Lower oxygen vacancies enhance the production of hydroxyl radicals on the surface of the electrode and hence the oxidizing ability. Gd covered the electrode surface with an increase in its content and reduced the availability of Sb (Feng et al. 2008). It is worth noting that not only the dopant, but also its content substantially influences the performance of an electrode.

Other dopants like La and Ru are also advantageous in modifying the characteristics of an electrode. On doping SnO_2-Sb with La and Ru, distortion effects led to the hindrance in the crystal growth and the crystallite size was reduced (Xu et al. 2012). The smaller crystallite size not only increases the surface area, but also increases the number of active sites on the surface of the anode. XPS measurements of this electrode revealed two different oxygen 1s peaks, one with lower binding energy (BE) component of 530.08–530.36 eV (assigned to lattice oxygen O_{lat}) incorporated into SnO_2 lattice and the other higher BE component of 531.86–531.89 eV (assigned to adsorbed oxygen O_{ads}) is of the weakly bonded oxygen species. The adsorbed oxygen is very reactive towards the oxidation of organics. The O_{ads} content on the surface of Ti/ SnO_2-Sb-La was found to be the highest (41.78 %), followed by Ti/SnO_2-Sb-Ru (39.42 %) and Ti/ SnO_2-Sb (29.13 %) electrodes. Evidently, the addition of La

and Ru as dopants substantially enhanced the performance of the Ti/SnO_2-Sb electrode in terms of COD removal and current efficiency (see Table 3).

Zhuo et al. (2011) reported that the service of Ti/SnO_2-Sb electrode doubled on doping with Bi. The degradation of perfluorooctanoic acid (PFOA) was successfully achieved (~90 %) on both Ti/SnO_2-Sb and Ti/SnO_2-Sb-Bi. Liu et al. (2013) have recently shown that the OER potential for the carbon nanotube (CNTs) coated with SnO_2 nanoparticles is higher than that of bulk SnO_2. A comparison was made between SnO_2 (TO-CNT), SnO_2-Sb (ATO-CNT), and SnO_2-Bi nanoparticle-coated CNT (BTO-CNT) for the electrochemical filtration of oxalate. SnO_2-Bi/CNT showed 1.5 to 3.5 times greater current efficiency and 4 to 5 times lesser energy consumption as compared to bare CNT for the electrooxidative filtration of ethanol, methanol, formaldehyde, and formate. Also, BTO-CNT showed higher OER potential and TOC removal as compared to ATO-CNT, suggesting that Bi can be an alternative for Sb. However, Lin et al. (2013a) reported that the Ti/SnO_2-Sb-Ce electrode yielded lower perfluorocarboxylic acid (PFCA) (perfluorononanoic acid (PFNA) and perfluorodecanoic acid (PFDA)) removal and observed secondary products of Sb due to the dissolution.

Modifications in the composition of SnO_2 electrode fabrication and investigation of their performance in the wastewater treatment are summarized in Table 3. The conditions used in the electrochemical wastewater treatment process, maximum COD/TOC removal achieved, and percent current efficiency have been summarized in this table. As mentioned earlier, the extent of degradation of an organic molecule is dependent on its chemical nature, structure, and stability. The data in Table 3 is helpful in selecting a particular electrode for the degradation of different organic pollutant and vice versa.

PbO_2

Generally, there are two kinds of PbO_2. Orthorhombic α-PbO_2 (brown color) and tetragonal β-PbO_2 (black color), where β-PbO_2 is a disordered close packed structure, possessing comparatively higher conductivity and higher overpotential for oxygen evolution are highly preferred (Abaci et al. 2005; Aquino et al. 2010; Gaber et al. 2012; Li et al. 2011; Yang et al. 2009; Zhoua and He 2008). β-PbO_2 is a non-active anode, highly conducting, chemically inert, cheaper than noble metals, and possesses high oxygen evolution overpotential and high catalytic activity for the production of oxidants. Direct oxidation of organics on the surface of PbO_2 anode is allowed (Fenga and Li 2003; Liu and Liu 2008; Yang et al. 2009). Thermal decomposition, electrodeposition (both in acidic and alkali media), and electrooxidation (anodization) are the techniques commonly employed in the fabrication of PbO_2 electrodes (Fenga and Li 2003; Liu and Liu 2008; Martínez-Huitle et al. 2008; Niu et al. 2012; Panizza and Cerisola 2008; Panizza and Cerisola 2009; Sala and Gutiérrez-Bouzán 2012; Soloman et al. 2009; Yang et al. 2009). Liu et al. (2009) have been able to fabricate both kinds of PbO_2 coat on Ti substrate. Pavlov (1992) carried out detailed work on the PbO_2 electrodes and proposed a complex mechanism of formation of hydroxyl radicals on the surface of lead dioxide anodes. A gel-crystal system was suggested which follows the equilibrium shown below (Liu et al. 2009; Pavlov 1992):

$$\underset{\text{Crystal layer}}{PbO_2} + H_2O \leftrightarrow \underset{\text{Hydrated(gel)layer}}{PbO(OH)_2} \leftrightarrow H_2PbO_3 \quad (14)$$

Precisely, according to Pavlov, in the gel zone, the hydrated PbO_2 forms linear polymer chains which allow the electron hopping from one Pb^{4+} ion to the other along the chain and from one polymer chain to the other, which accounts for its conductivity. The crystal zone is made up of PbO_2 and allows electrical conductivity. There exists certain number of active centers on the surface of the PbO_2 crystal layer. The hydroxide ions in the solution give out the electrons to these active centers which lead to the formation of hydroxyl radicals and create a weak interactive bond with the active centers. These hydroxyl radicals are utilized in the oxidation of organics (Liu et al. 2009).

PbO_2 as itself has been used in the electrochemical treatment of wastewater and also in its doped form. On adding suitable dopant, PbO_2 exhibits exceptional electrochemical properties. Ni, Bi, Co, Er, and Ce are the most commonly used dopants (Yang et al. 2009; Liu and Liu 2008; Liu et al. 2009; Niu et al. 2012; Wang et al. 2010b). Niobium-doped PbO_2 has showed excellent hydrophilicity and conductivity due to the improvement in its microcrystal structure (Yang et al. 2009). It has also been reported that doping roughened the thin film surface and increased the effective surface area for the generation of hydroxyl radicals (Yang et al. 2009). The effect of bismuth and cobalt as dopants in the fabrication of PbO_2 by electrodeposition was studied by Liu et al. (2009) and Liu and Liu (2008). This electrode was used in the degradation of nitrophenols. The addition of bismuth into the PbO_2 matrix remarkably decreased the crystallite size of the deposit and improved its electrocatalytic activity. Out of Ti/β-PbO_2, Ti/Bi-PbO_2, Ti/Co-PbO_2, Ti/Bi-Co-PbO_2 electrodes, the morphology of Ti/Bi-PbO_2 was found to be compact and porous with small crystallite size. This was attributed to the variations caused by the formation of Bi_2O_5 in the nucleation and crystal growth of the film (Liu and Liu 2008; Liu et al. 2009). In addition, this anode showed the highest oxygen evolution overpotential of 1.75 V (vs. SCE) and stability. Ti/Bi-PbO_2 and Ti/Bi-Co-PbO_2 favored the generation of hydrogen peroxide and hypochlorite ion. In contrast, no effect on the PbO_2 crystallite size was found by doping cobalt. Ti/Bi-PbO_2 showed the highest electrocatalytic activity

for the generation of $^{\bullet}OH$. Obviously, the COD removal was maximum in the case of Ti/Bi-PbO_2. Though Ti/Bi-Co-PbO_2 exhibited smallest removal rates, its current efficiency was higher than Ti/β-PbO_2 and Ti/Co-PbO_2. Thus, Bi doping into the PbO_2 matrix dramatically improves its characteristics, but Co doping does not make any such differences.

Similar influence of doping was observed when Er was used as dopant. The Er doping into F-PbO_2 improved the electrocatalytic activity and produced compact coating with decreased crystallite size. Wang et al. (2010b) prepared erbium-doped chitosan-F-PbO_2 electrode and compared it with the electrode without Er doping and without chitosan for the degradation of 2,4-dichlorophenol (2,4-DCP). Maximum 2,4-DCP removal was achieved on the electrode obtained from 10 mM Er electroplating solution. The order of 2,4-DCP removal on different electrodes was found to be Ti/SnO_2-Sb_2O_3/Er-chitosan-F-PbO_2 > Ti/SnO_2-Sb_2O_3/Er-F-PbO_2 > Ti/SnO_2-Sb_2O_3/F-PbO_2.

PbO_2 was electrodeposited on Ti/SnO_2-Sb(0.08) (8 mol % of Sb) interlayer using different concentrations of NaF in the electrodeposition bath solution (Mao et al. 2008). The NaF concentration not only affected the stability of PbO_2, but also the morphology of the PbO_2 deposit. Without the addition of NaF, the PbO_2 coat obtained consisted irregular crystallite size and shape with dents of varying sizes on the surface. As the concentration of NaF increased, a more compact coat of PbO_2 was obtained. Only 55 % color removal of the substrate AO7 was achieved on PbO_2-F (0.75) electrode, whereas PbO_2-F (0) showed 94 % removal for the same time period. This was attributed to more compact and uniform deposition which resulted with the inclusion of NaF. The higher color removal in case of PbO_2-F (0.75) electrode is due to the rough surface area which facilitated the adsorption of dye. With 0.1 g L^{-1} of NaF (PbO_2-F (0.1)), the PbO_2 coat obtained was most stable to anodic dissolution in 1 M $HOCl_4$ (Mao et al. 2008). β-PbO_2 coated on Ti with SnO_2-Sb_2O_3-Nb_2O_5 interlayer showed higher electrochemical activity than Ti/RuO_2 and Ti/Sb-Sn-RuO_2 anodes for the degradation of phenol. The interlayer enhanced the surface area, electrocatalytic activity, conductivity, and hence the efficiency. Evidently, the removal efficiency increased from 78.6 % (Na_2SO_4) to 97.2 % on adding 21.3 g L^{-1} of NaCl.

Niu et al. (2012) reported that the toxic PFCAs like perfluorobutanoic acid (PFBA), PFPA, PFHxA, PFHpA, and PFOA, which are recently driving attention as serious contaminants in various environmental matrices, can be successfully mineralized by electrochemical method using Ce-doped porous nanocrystalline PbO_2 film electrode (Ti/SnO_2-Sb/PbO_2-Ce). The same electrode provided excellent mineralization of PFNA, PFDA, and sulfamethoxazole as reported by Lin et al. (2013a, b) under mild conditions.

The dissolution of PbO_2 in strong basic conditions and on specific anodic polarization limits its usage in wastewater treatment (Carvalho et al. 2011; Niu et al. 2012). However, by adopting suitable fabrication technique, the wear resistance of PbO_2 can be conditioned (Carvalho et al. 2011) and possible release of Pb^{2+} in acidic conditions can be avoided by the application of suitable anodic current (Niu et al. 2012). Unlike SnO_2, passivation of surface due to the formation of hydroxides is avoided by the continuous production of hydroxyl radicals on the surface of PbO_2 and offers high charge transfer. Table 4 summarizes the comparison between the various modified PbO_2 anodes and conditions used in the electrochemical wastewater treatment process.

Ruthenium oxide and iridium oxide

RuO_2- and IrO_2-based anodes are active anodes, known for their electrocatalytic activity for oxygen and chlorine evolution. IrO_2 is one of the cheapest dimensionally stable anodes and shows low chlorine and oxygen evolution overpotential used in the generation of active chlorine species (Zaviska et al. 2009). Both IrO_2- and RuO_2-coated Ti anodes undergo dissolution in basic medium on anodization (Li et al. 2009). Ti/RuO_2 undergoes corrosion during electrolysis on prolonged usage (Papastefanakis et al. 2010). However, the service life of RuO_2 enhances on doping with Ir (Chandler et al. 1997; Chen et al. 2001, 2002; Duby 1993; Nikolić et al. 2012). The electrochemical properties of iridium ($Ti_{0.6}Ir_{0.4}O_2$/Ti) and ruthenium ($Ti_{0.6}Ru_{0.4}O_2$/Ti) oxide anodes, prepared by sol–gel method, were investigated by Panić et al. (2003a, b, 2007, 2010). They found that the iridium oxide shows enhanced catalytic activity for both oxygen and chlorine evolution and stability against corrosion as compared to ruthenium oxide (Panić et al. 2003a, b, 2007, 2010). These electrodes provide only small range of operating potential within hydrogen and oxygen evolution reactions. It is difficult to realize the direct oxidation of variety of organics on these anodes within this potential range. Hence, practical relevance of these anodes in the wastewater treatment on large scale is unacceptable. However, few research teams have successfully degraded the organic pollutants using these anodes.

The low chlorine evolution overpotential on these anodes is advantageous in the production of active chlorine species in wastewater containing chloride ions. The addition of NaCl as supporting electrolyte improves the removal efficiency, indicating that electrochemical treatment using Ti/IrO_2 and Ti/RuO_2 involves both direct and indirect oxidation (Chatzisymeon et al. 2009; Li et al. 2009). Enhancement in the COD removal efficiency was observed due to oxidation mediated by the electrochemically generated oxidants in the presence of chloride ions using Ti/RuO_2 anode in olive mill wastewater treatment (Papastefanakis et al. 2010). The degradation process involved the formation of intermediates followed by further oxidation to CO_2 and water.

Table 5 Performance of different modified RuO_2 and IrO_2 anodes and working conditions

Pollutant	Electrode	Operating conditions	% COD and TOC removal, %CE, TEC	Remarks	Reference
	IrO_2-Ta_2O_5			OER potential=1.5–1.8 V	Kapałka et al. (2008)
Phenol-formaldehyde	1. Ti/$Ru_{0.3}Ti_{0.7}O_2$	Phenol–IC=0.425 mmol L^{-1}, formaldehyde= 67.000 mmol L^{-1}, SE: NaCl (1.000 mol L^{-1}) pH–5.5, j=40	TOC=68	Effect of Na_2SO_4 and $NaNO_3$ as supporting electrolytes was investigated. But removal efficiency was found to be highest in the presence of NaCl. Electrode is wear resistant	Fornazari et al. (2012)
Methyl violet (MV2B)	1. Ti/IrO_2	IC=50 mg L^{-1}, SE=3.42 mM, FR=2 L min^{-1}, j=15	COD=62.7±3.7 (initial in mg L^{-1}), COD=15.7±0.0 (final in mg L^{-1}), TOC=40.6±4.5 (initial in mg L^{-1}), TOC=19.8±0.6 (final in mg L^{-1}), instantaneous %CE=41.3±3.3	The removal efficiency increased with the chloride concentration and current density, but decreased with the increase in the initial concentration of the dye and flow rate. Trypan blue was most resilient to degradation	Zaviska et al. (2009)
Trypan Blue		IC=48.6 mg L^{-1}	COD=27.4 (initial in mg L^{-1}) COD=20.9 (final in mg L^{-1}), instantaneous %CE=5.7		
Acridine		IC=51.6 mg L^{-1}	COD=35.3 (initial in mg L^{-1}) COD=17.0 (final in mg L^{-1}), instantaneous %CE=16.1		
Eosin Yellow		IC=49.3 mg L^{-1}	COD=22.2 (initial in mg L^{-1}) COD=2.6 (final in mgL^{-1}), instantaneous %CE=17.2		
Reactive blue 81 Reactive Red 2	1. Ti/$TiO_{2(70\ \%)}$–$RuO_{2(30\ \%)}$	IC=0.5 g L^{-1} (60 mL), 2 h, SE: $NaClO_4$ (0.1 mol L^{-1}), appl. voltage=0.9 V	TOC=13, COD=18 TOC=14, COD=39	Complete mineralization was achieved with irradiation (wavelength 254 nm) and j=20 mA cm^{-2}	Kusmierek et al. (2011)
Alphazurine dye	1. Ti/IrO_2	IC=500 mg L^{-1}, SE: Na_2SO_4, j=30	COD=60, %CE=3, TEC=254	Oxidation of alphazurine was slow as compared to oxygen evolution reaction (OER=1.3 V vs SCE)	Nava et al. (2008)
Olive mill wastewater	1. Ti/RuO_2	1 M $HClO_4$, 80 °C, 5 h, j=50	COD=52, TOC=38	Charge consumed=28 Ah L^{-1}. Addition of 20 mM NaCl enhanced the COD removal by 8 times	Papastefanakis et al. (2010)
Olive mill wastewater	1. Ti/IrO_2	1 M $HClO_4$ 80 °C, j=50	COD=60, total phenolic compound removal=85	COD removal increased with current density. Variation in temperature influenced the removal efficiency. Addition of 5 mM NaCl enhanced the COD removal. Formation of toxic organochlorinated by-products was observed	Chatzisymeon et al. (2009)

Table 5 (continued)

Pollutant	Electrode	Operating conditions	% COD and TOC removal, %CE, TEC	Remarks	Reference
Reactive Red 120	1. Ti/IrO_2-RuO_2	120 mL, 1 M $HClO_4$, 5 h	TOC=10 (25 °C), TOC=40 (80 °C), COD=43 (j=50 mA cm^{-2}), COD=32 (j=15 mA cm^{-2}), instantaneous %CE=13	Only selective oxidation occurred. COD removal reached up to 60 % after supplying 26 Ah L^{-1} charge	Panakoulias et al. (2010)
Phenol	1. Ti/IrO_2-Pt	IC=8 mg L^{-1}, SE=0.3 mg L^{-1}, NaCl 50 min, j=10	TOC=100	OER potential 1.2 V vs SCE. The TOC removal rate increased with current density	Li et al. (2009)
	2. Ti/RuO_2-Pt	IC=8 mg L^{-1}, SE=0.3 g L^{-1}, NaCl 30 min, j=10	TOC=100	OER potential 1.58 V vs SCE	
Oxalic acid	1. IrO_2-Ta_2O_5	IC=0.1 M, FR=1.2 L min^{-1}, 25 °C, j=17	COD=91 to 95, instantaneous %CE=62 to 66	The duration for complete mineralization was monitored (778 min). The removal rate increased with flow rate of the sample and applied current density	Scialdone et al. (2009a)
		IC=0.1 M, FR=0.2 L min^{-1}, SE=5 g L^{-1} NaCl, 25 °C, j=39	COD=>98, instantaneous %CE=71 to 75	Time elapsed=334 min	
		IC=0.1 M, FR=1.2 L min^{-1}, 50 °C, j=17	COD=>99, instantaneous %CE=68 to 72	Time elapsed=778 min	
Reactive Blue 4	1. $Ti/(RuO_2)_{0.7}$-$(Ta_2O_5)_{0.30}$	IC=100 mg L^{-1} (50 mL), SE=Na_2SO_4, j=50	TOC=20	The COD removal increased from 30 to 80 % in the presence of chloride ions. The formation of toxic AOX was observed with all 3 electrodes. Ru and Ta electrode although displayed slowest oxidation rates, the amount of AOX formed was low	da Silva et al. (2011)
	2. $Ti/Ru_{0.30}Ti_{0.70}O_2$		TOC=38, instantaneous %CE=3 to 6		
	3. $Ti/Ru_{0.30}Sn_{0.70}O_2$		TOC=28		
Reactive Orange 16	1. $Ti/(RuO_2)_{0.70}$-$(Ta_2O_5)_{0.30}$		TOC- 22		
	2. $Ti/Ru_{0.30}Ti_{0.70}O_2$		TOC=32		
	3. $Ti/Ru_{0.30}Sn_{0.70}O_2$		TOC=27		
Reactive Brilliant Red K-2BP	Ti/RuTiIrSnMn oxide	100 mg L^{-1} (200 mL), j=30, FR=50 mL min^{-1}, SE: NaCl (0.4 g L^{-1})		Degradation of brilliant red K-2BP was improved in the presence of NaCl on Ti/RuTiIrSnMn electrode at lower pH and higher temperatures	Jiancheng et al. (2012)

IC initial concentration of the pollutant, *SE* supporting electrolyte, *j* current density (in milliamperes per square centimeter), *FR* electrolyte flow rate in case of recirculation batch systems, *%ICE* instantaneous percentage current efficiency, *TEC* total energy consumed (in kilowatt-hours per cubic meter)

Due to high electrocatalytic activity and stability, IrO_2-Ta_2O_5 anode finds wide industrial applications (Scialdone et al. 2009a). IrO_2-Ta_2O_5 anode is known for its selective oxidation. It oxidizes the organics into simpler carboxylic acids, particularly oxalic acid (Scialdone et al. 2009a). IrO_2-Ta_2O_5 is the suitable electrode for the degradation of OA (Scialdone et al. 2009a; Ferro et al. 2010).

Three different DSA®s, Ti/$(RuO_2)_{0.70}(Ta_2O_5)_{0.30}$, Ti/$Ru_{0.30}Ti_{0.70}O_2$, and Ti/$Ru_{0.30}Sn_{0.70}O_2$, were used in the degradation of RB-4 and RO-16 (da Silva et al. 2011). The Ti/$Ru_{0.30}Ti_{0.70}O_2$ showed the highest current efficiency among these electrodes. Indirect electrochemical oxidation by the active chlorine species generated in presence of NaCl enhanced the COD removal on this electrode. Ti/$Ru_{0.30}Ti_{0.70}O_2$ anode showed higher OER potential as compared to the other two. The same electrode was used in the degradation of Reactive Blue 81 and Reactive Red 2 by Kusmierek et al. (2011). Complete mineralization was achieved when the electrochemical degradation was coupled with the UV irradiation. These results indicate that TiO_2-RuO_2 mixed metal oxide solid solution is effective in the generation of active chlorine species. As these dyes can be successfully mineralized by indirect electrochemical oxidation, Ti/$Ru_{0.30}Ti_{0.70}O_2$ anode is suitable for the treatment of wastewater containing these dyes.

Chu et al. (2010) prepared Ti/RuO_2/IrO_2/TiO_2 with two compositions: one electrode (#1) with 0.20, 0.85, and 0.40 mg cm^{-2} of Ru, Ir and Ti, respectively, whereas the other electrode (#2) composed of 1.10, 1.20, and 0.55 mg cm^{-2} of Ru, Ir, and Ti, respectively. The higher oxide loading in case of #2 led to relatively rough surface of the coating. Direct oxidation of 2,4-DCP was observed on this electrode (Chu et al. 2010). Pt doping increases the service life of IrO_2 and RuO_2 anodes and the inability of Pt to produce hydroxyl ions is compensated by the ruthenium and/or iridium oxides (Li et al. 2009).

Table 5 compares different modified RuO_2 and IrO_2 anodes. The conditions used in the electrochemical wastewater treatment process, COD and TOC removal, and current efficiency displayed are useful in comparing the affinity of electrodes for different pollutant molecules.

Comparison between main metal oxide anodes

Table 6 reveals that the potential corresponding to the commencement of oxygen evolution reaction on the anode is related to OER overpotential and adsorption enthalpy of hydroxyl radicals (Kapałka et al. 2008). The ability of the anode to oxidize the organics increases with an increase in OER overpotential. Evidently, IrO_2 and RuO_2 are active anodes with low OER overpotential and are best suited for the production of chlorine and oxygen in chlor-alkali industries and electroorganic synthesis. They provide only partial decontamination with high energy consumption. The OER is highest for SnO_2 anode, and hence, it possesses high electrocatalytic activity for the production of hydroxyl radicals. Therefore, complete incineration of organics is viable. Similarly, OER for PbO_2 is also considerable and it is only slightly less than that of SnO_2. The only problem encountered in the implementation of these anodes for the wasterwater treatment on large scale is their dissolution on electrolysis in severe wastewater matrix. Studies on appropriate modifications in the fabrication technique to enhance their stability are of much importance.

BDD anode recognized as the highly efficient anode for the oxidative degradation of organics in the past few years has acquired a lot of attention. Hydroxyl radical adsorption is very weak on the surface of BDD. The potential window between OER (2.2–2.6 V) and hydrogen evolution reaction is wide (>3 V) (Brillas et al. 2009; Koparal et al. 2007; Martínez-Huitle and Ferro 2006; Panizza and Cerisola 2008). However, BDD fabrication is very expensive as compared to metal oxide anodes. If appropriate modifications of metal oxide anodes to meet the characteristics of BDD and operating conditions are optimized to stretch the performance to the maximum, it only takes a mere part of the cost to achieve the same effectiveness as on BDD.

Conclusion

The electrochemical oxidation involving metal oxide electrodes for the abatement of organics in wastewater is an effective tool to keep up the aesthetic and environmental health. Nature of the electrode, pollutant, and operating conditions should coordinate suitably to successfully accomplish the goal of complete elimination of

Table 6 Oxidation power of the anode material in acid media

Adapted from Kapałka et al. (2008) and Martínez-Huitle and Andrade (2011). Standard potential for oxygen evolution is 1.23 V vs normal hydrogen electrode

Electrode	Oxidation potential/V	Overpotential for oxygen evolution/V
RuO_2-TiO_2 (DSA-Cl_2)	1.4–1.7	0.18
IrO_2-Ta_2O_5 (DSA-O_2)	1.5–1.8	0.25
Ti/PbO_2	1.8–2.0	0.50
Ti/SnO_2-Sb_2O_5	1.9–2.2	0.70

organics. The physical and chemical properties of the electrodes can be tuned by adopting appropriate fabrication technique to serve their purpose.

The structure, size, alignment, and morphology of the coated oxide thin film command the mechanism followed by the electrode. Electrodes with smooth surface interact very weakly with the hydroxyl radicals, and hence, these radicals are available for the oxidation of the organics, whereas on the electrodes with small crystallite size, large and rough surface areas provide sites for the hydroxyl radicals and organic molecules to adsorb strongly. The availability of hydroxyl radicals for the oxidation of organics diminishes on strong adsorption. Furthermore, with an increase in active centers on the surface of the oxide electrode and applied current density, the rate of formation of hydroxyl radicals also increases. Hence, metal oxide electrodes with smooth surface, small crystallite size, and high surface area are more effective. These prerequisite properties can be furnished with the help of suitable alterations made during the fabrication of the electrode. Selection of proper fabrication method, doping agent, interlayer insertion, and composition can bring out the best results.

Indirect oxidation of organics by the electrochemically generated oxidants is also a best method. Chloride is the most favorite electrolyte and ClO_4^-, NO_3^-, PO_4^{2-}, SO_4^{2-}, CO_3^{2-}, and Br^- are also effective under appropriate optimized operating conditions. Inclusion of chloride ions substantially enhanced the efficiency in color, COD, and TOC removal in many cases due to the formation of HOCl, ClO^-, and Cl_2. However, the risk of formation of AOX should be considered. Sulfate radicals, peroxydisulfate, peroxydicarbonate, and peroxydiphospates are also strong oxidants and can be effective under suitable conditions.

Among the three main metal oxide anodes discussed in this review, IrO_2 and RuO_2 show lowest OER potential. The oxygen evolution reaction on these electrodes competes with the oxidation reaction of organics. The complete removal of organics using these electrodes is possible only by indirect electrochemical oxidation. However, these electrodes are best suited for Cl_2 generation and electroorganic synthesis. Both SnO_2 and PbO_2 exhibit very good electrochemical activity for the oxidation of organics and electrocatalytic activity for the production of hydroxyl radicals. The service life of PbO_2 is greater than that of SnO_2, and the OER for SnO_2 is higher than that of PbO_2. Metal dissolution is a serious concern in electrochemical treatment process. SnO_2-Sb, PbO_2, IrO_2, and RuO_2 electrodes undergo dissolution in basic medium and high anodic potentials. However, modified SnO_2 and PbO_2 electrodes show high stability, electrochemical, and electrocatalytic properties than modified IrO_2 or RuO_2 electrodes. The performance of SnO_2 and PbO_2 is comparable with the BDD electrode which is recognized as a highly efficient anode for the oxidative degradation of organics. This makes modified SnO_2 and PbO_2 electrodes as suitable candidates for the electrochemical wastewater treatment on large scale.

Acknowledgments We thank the Department of Chemistry, Kuvempu University, Shankaraghatta for their support.

References

Abaci S, Tamer U, Pekmez K, Yildiz A (2005) Performance of different crystal structures of PbO_2 on electrochemical degradation of phenol in aqueous solution. Appl Surf Sci 240:112–119

Amjoud M'B, Maury F, Soukane S, Duverneuil P (1998) Making of specific electrodes by CVD. Surf Coat Technol 100–101:169–172

Andrade LS, Tasso TT, da Silva DL, Rocha-Filho RC, Bocchi N, Biaggio SR (2009) On the performances of lead dioxide and boron-doped diamond electrodes in the anodic oxidation of simulated wastewater containing the Reactive Orange 16 dye. Electrochim Acta 54:2024–2030

Aquino JM, Rocha-Filho RC, Bocchi N, Biaggio SR (2010) Electrochemical degradation of the Acid Blue 62 dye on a b-PbO_2 anode assessed by the response surface methodology. J Appl Electrochem 40:1751–1757

Attia SM, Wang J, Wu G, Shen J, Ma J (2002) Review on sol–gel derived coatings: process, techniques and optical applications. J Mater Sci Technol 18(3):211–214

Beer HB (1980) The invention and industrial development of metal. Reviews and news. J Electrochem Soc 127(8): 303C–307C

Brillas E, Sires I, Oturan MA (2009) Electro-Fenton process and related electrochemical technologies based on Fenton's reaction chemistry. Chem Rev 109:6570–6631

Brinker CJ, Frye GC, Hurd AJ, Ashley CS (1991) Fundamentals of sol–gel dip coating. Thin Solid Films 201:97–108

Brungs A, Haddadi-Asl V, Skyllas-Kazacos M (1996) Preparation and evaluation of electrocatalytic oxide coatings on conductive carbon-polymer composite substrates for use as dimensionally stable anode. J Appl Electrochem 26:1117–1123

Carvalho DA, Rocha JHB, Fernandes NS, da Silva DR, Martínez-Huitle CA (2011) Application of electrochemical oxidation as alternative for removing methyl green dye from aqueous solutions. Latin Am Appl Res 41:127–133

Chandler GK, Genders JD, Pletcher D (1997) Electrodes based on noble metals—essential components for electrochemical technology. Platinum Met Rev 41(2):54–63

Chatzisymeon E, Dimou A, Mantzavinos D, Katsaounis A (2009) Electrochemical oxidation of model compounds and olive mill wastewater over DSA® electrodes: 1. The case of Ti/IrO_2 anode. J Hazard Mater 167:268–274

Chen X, Chen G, Yue PL (2001) Stable Ti/IrOx-Sb_2O_5-SnO_2 anode for O_2 evolution with low Ir content. J Phys Chem B 105:4623–4628

Chen G, Chen X, Yue PL (2002) Electrochemical behavior of novel Ti/IrOx-Sb_2O_5-SnO_2 anodes. J Phys Che B 106:4364–4369

Cheng-chun J, Jia-fa Z (2007) Progress and prospect in electro-Fenton process for wastewater treatment. J Zhejiang Univ Sci A 8(7): 1118–1125

Choi H, Stathatos E, Dionysiou DD (2007) Photocatalytic TiO_2 films and membranes for the development of efficient wastewater treatment and reuse systems. Desalination 202:199–206

Chu YY, Wang WJ, Wang M (2010) Anodic oxidation process for the degradation of 2,4-dichlorophenol in aqueous solution and the enhancement of biodegradability. J Hazard Mater 180:247–252

Comninellis C (1994) Electrocatalysis in the electrochemical conversion/combustion of organic pollutants for wastewater treatment. Electrochem Acta 39:1857–1862

Comninellis Ch, Chen G (2010) Electrochemistry for the environment. Springer, Berlin. doi:10.1007/978-0-387-68318-8

Comninellis C, Vercesi GP (1991) Characterization of DSA®-type oxygen evolving electrodes: choice of a coating. J Appl Electrochem 21:335–345

Correa-Lozano B, Comninellis C, de Battisti A (1996a) Preparation of SnO_2–Sb_2O_5 films by the spray pyrolysis technique. J Appl Electrochem 26:83–89

Correa-Lozano B, Comninellis C, de Battisti A (1996b) Electrochemical properties of Ti/SnO_2-Sb_2O_5 electrodes prepared by the spray pyrolysis technique. J Appl Electrochem 26(7):683–688

Correa-Lozano B, Comninellis C, De Battisti A (1997) Service life of Ti/SnO_2-Sb_2O_5 anodes. J Appl Electrochem 27:970–974

Costa CR, Montilla F, Morallón E, Olivi P (2010) Electrochemical oxidation of synthetic tannery wastewater in chloride-free aqueous media. J Hazard Mater 180:429–435

da Silva RG, Neto SA, De Andrade AR (2011) Electrochemical degradation of reactive dyes at different DSA® compositions. J Braz Chem Soc 22(1):126–133

del Río AI, Molina J, Bonastre J, Cases F (2009) Study of the electrochemical oxidation and reduction of C.I. Reactive Orange 4 in sodium sulfate alkaline solutions. J Hazard Mater 172:187–195

Devilliers D, Dinh Thi MT, Mahé E, Le Xuan Q (2003) Cr(III) oxidation with lead dioxide-based anodes. Electrochim Acta 48:4301–4309

Duby P (1993) The history of progress in dimensionally stable anodes. JOM 45(3):41–43

Duverneuil P, Maury F, Pebere N, Senocq F, Vergnes H (2002) Chemical vapor deposition of SnO2 coatings on Ti plates for the preparation of electrocatalytic anodes. Surf Coat Technol 151 –152:9–13

Fachinotti E, Guerrini E, Tavares AC, Trasatti S (2007) Electrocatalysis of H_2 evolution by thermally prepared ruthenium oxide effect of precursors: nitrate vs. chloride. J Electroanal Chem 600:103–112

Feng Y, Cui Y, Logan B, Liu Z (2008) Performance of Gd-doped Ti-based Sb-SnO2 anodes for electrochemical destruction of phenol. Chemosphere 70:1629–1636

Fenga YJ, Li XY (2003) Electro-catalytic oxidation of phenol on several metal-oxide electrodes in aqueous solution. Water Res 37:2399–2407

Ferro S, Martínez-Huitle CA, De Battist A (2010) Electroxidation of oxalic acid at different electrode materials. J Appl Electrochem 40:1779–1787

Fierro S, Comninellis C (2010) Kinetic study of formic acid oxidation on Ti/IrO_2 electrodes prepared using the spin coating deposition technique. Electrochim Acta 55:7067–7073

Fornazari ALT, Malpass GRP, Miwa DW, Motheo AJ (2012) Application of electrochemical degradation of wastewater composed of mixtures of phenol–formaldehyde. Water Air Soil Pollut 223:4895–4904

Gaber M, Ghalwa NA, Khedr AM, Salem MF (2012) Electrochemical degradation of reactive yellow160 dye in real wastewater using C/PbO_2-, Pb + Sn/PbO2 + SnO2-, and Pb/PbO_2 modified electrodes. J Chem 2013:1–9

Guinea E, Brillas E, Centellas F, Cañizares P, Rodrigo MA, Sáez C (2009) Oxidation of enrofloxacin with conductive-diamond electrochemical oxidation, ozonation and Fenton oxidation: a comparison. Water Res 43:2131–2138

He D, Mho S (2004) Electrocatalytic reactions of phenolic compounds at ferric ion co-doped SnO_2:Sb^{5+} electrodes [J]. J Electroana Chem 568:19–27

Hou Y, Qu J, Zhao X, Lei P, Wan D, Huang CP (2009) Electrophotocatalytic degradation of acid orange II using a novel TiO_2/ACF photoanode. Sci Total Environ 407:2431–2439

Jiancheng L, Jie Y, Weishan L, Qiming H, Hongkang X (2012) Electrochemical degradation of Reactive Brilliant Red K-2BP on Ti/RuTiIrSnMn oxide anode in a batch cell. J Electrochem Sci Eng 2:171–183. doi:10.5599/jese.2012.0022

Jiang-tao K, Shao-yuan S, Xiu-ping Z, Jin-ren N (2007) Effect of Sb dopant amount on the structure and electrocatalytic capability of Ti/Sb-SnO_2 electrodes in the oxidation of 4-chlorophenol. J Environ Sci 19:1380–1386

Jüttner K, Galla U, Schmieder H (2000) Electrochemical approaches to environmental problems in the process industry. Electrochim Acta 45:2575–2594

Kapałka A, Fóti G, Comninellis C (2008) Kinetic modelling of the electrochemical mineralization of organic pollutants for wastewater treatment. J Appl Electrochem 38:7–16

Klamklang S, Vergnes H, Pruksathorn K, Damronglerd S (2012) Electrochemical incineration of organic pollutants for wastewater treatment: Past, present and prospect. In: Puzyn T, Mostrag-Szlichtyng A (eds) Organic pollutants ten years after the Stockholm convention – Environmental and Analytical update. doi:10.5772/1381. Available from: http://www.intechopen.com/books/organic-pollutants-ten-years-after-the-stockholm-convention-environmental-and-analytical-update/electrochemical-incineration-of-organic-pollutants-for-wastewater-treatment-past-present-and-prospec. Accessed Aug 2013

Kong H, Lu H, Zhang W, Lin H, Huang W (2012) Performance characterization of Ti substrate lead dioxide electrode with different solid solution interlayers. J Mater Sci 47:6709–6715

Koparal AS, Yavuz Y, Gürel C, Öğütveren UB (2007) Electrochemical degradation and toxicity reduction of C.I. Basic Red 29 solution and textile wastewater by using diamond anode. J Hazard Mater 145:100–108

Kusmierek E, Chrzescijanska E, Szadkowska-Nicze M, Kaluzna-Czaplinska J (2011) Electrochemical discolouration and degradation of reactive dichlorotriazine dyes: reaction pathways. J Appl Electrochem 41:51–62

Li M, Feng C, Hu W, Zhang Z, Sugiura N (2009) Electrochemical degradation of phenol using electrodes of Ti/RuO_2–Pt and Ti/IrO_2–Pt. J Hazard Mater 162:455–462

Li X, Pletcher D, Walsh FC (2011) Critical review: electrodeposited lead dioxide coatings. Chem Soc Rev 40:3879–3894

Lin H, Niu J, Xu J, Huang H, Li D, Yue Z, Feng C (2013a) Highly efficient and mild electrochemical mineralization of long-chain perfluorocarboxylic acids (C9 C10) by Ti/SnO2-Sb-Ce, Ti/SnO2-Sb/Ce-PbO2 and Ti/BDD electrodes. Environ Sci Technol. doi:10.1021/es4034414

Lin H, Niu J, Xu J, Li Y, Pan Y (2013b) Electrochemical mineralization of sulfamethoxazole by Ti/SnO2-Sb/Ce-PbO2 anode: kinetics, reaction pathways, and energy cost evolution. Electrochim Acta 97:167–174

Lipp L, Pletcher D (1997) The preparation and characterization of tin dioxide coated titanium electrodes. Electrochim Acta 42(7):1091–1099

Liu Y, Liu H (2008) Comparative studies on the electrocatalytic properties of modified PbO_2 anodes. Electrochim Acta 53:5077–5083

Liu Y, Liu H, Ma J, Wang X (2009) Comparison of degradation mechanism of electrochemical oxidation of di- and tri-nitrophenols on Bi-doped lead dioxide electrode: effect of the molecular structure. Appl Catal B 91:284–299

Liu H, Vajpayee A, Vecitis CD (2013) Bismuth-doped tin oxide-coated carbon nanotube network: improved anode stability and efficiency

for flow-through organic electrooxidation. Appl Mater Interfaces. doi:10.1021/am402621v

Lu PJ, Chien CW, Chen TS, Chern JM (2010) Azo dye degradation kinetics in TiO_2 film-coated photoreactor. Chem Eng J 163:28–34

Malpass GRP, Miwa DW, Santos RL, Vieira EM, Motheo AJ (2012) Unexpected toxicity decrease during photoelectrochemical degradation of atrazine with NaCl. Environ Chem Lett 10:177–182

Mao X, Tian F, Gan F, Lin A, Zhang X (2008) Comparison of the performances of Ti/SnO2–Sb, Ti/SnO2–Sb/PbO2 and Nb/BDD anodes on electrochemical degradation of azo dye. Russ J Electrochem 44:802–811

Martínez-Huitle CA, Andrade LS (2011) Electrocatalysis in wastewater treatment: recent mechanism advances. Quim Nova 34(5):850–858

Martínez-Huitle CA, Brillas E (2009) Decontamination of wastewaters containing synthetic organic dyes by electrochemical methods: a general review. Appl Catal B Environ 87:105–145

Martínez-Huitle CA, Ferro S (2006) Electrochemical oxidation of organic pollutants for the wastewater treatment: direct and indirect processes. Chem Soc Rev 35:1324–1340

Martínez-Huitle CA, de Battisti A, Ferro S, Reyna S, Cerro-López M, Quiro MA (2008) Removal of the pesticide methamidophos from aqueous solutions by electrooxidation using Pb/PbO2, Ti/SnO2, and Si/BDD electrodes. Environ Sci Technol 42:6929–6935

Marugán J, López-Muñoz MJ, van Grieken R, Aguado J (2007) Photocatalytic decolorization and mineralization of dyes with nanocrystalline TiO_2/SiO_2 materials. Ind Eng Chem Res 46:7605–7610

Nava JL, Quiroz MA, Martínez-Huitle CA (2008) Electrochemical treatment of synthetic wastewaters containing alphazurine A dye: role of electrode material in the colour and COD removal. J Mex Chem Soc 52(4):249–255

Nikolić BŽ, Panić VV, Dekanski AB (2012) Intrinsic potential-dependent performances of a sol–gel prepared electrocatalytic IrO_2–TiO_2 coating of dimensionally stable anodes. Ectrocatalysis 3:360–368

Niu J, Lin H, Xu J, Wu H, Li Y (2012) Electrochemical mineralization of perfluorocarboxylic acids (PFCAs) by Ce-doped modified porous nanocrystalline PbO2 film electrode. Environ Sci Technol 46: 10191–10198

Ozer N, DeSouza S, Lampert CM (1995) Optical and electrochemical properties of sol–gel spin coated CeO_2-TiO_2 films. SPIE 2531:143

Panakoulias T, Kalatzis P, Kalderis D, Katsaounis A (2010) Electrochemical degradation of Reactive Red 120 using DSA and BDD anodes. J Appl Electrochem 40:1759–1765

Panić VV, Nikolić BŽ (2007) Sol–gel prepared active ternary oxide coating on titanium in cathodic protection. J Serb Chem Soc 72(12):1393–1402

Panić V, Vidaković T, Gojkovic S, Dekanski A, Milonjić S, Nikolić B (2003a) The properties of carbon-supported hydrous ruthenium oxide obtained from RuO_xH_y sol. Electrochim Acta 48:3805–3813

Panić V, Dekanski A, Wang G, Fedoroff M, Milonjić S, Nikolić B (2003b) Morphology of RuO_2–TiO_2 coatings and TEM characterization of oxide sols used for their preparation. J Colloid Interface Sci 263:68–73

Panić VV, Dekanski AB, Mišković-Stanković VB, Milonjić SK, Nikolić BŽ (2010) Differences in the electrochemical behavior of ruthenium and iridium oxide in electrocatalytic coatings of activated titanium anodes prepared by the sol–gel procedure. J Serb Chem Soc 75(10): 1413–1420

Panizza M, Cerisola G (2008) Electrochemical degradation of methyl red using BDD and PbO_2 anodes. Ind Eng Chem Res 47:6816–6820

Panizza M, Cerisola G (2009) Direct and mediated anodic oxidation of organic pollutants. Chem Rev 109:6541–6569

Panizza M, Cerisola G (2010) Applicability of electrochemical methods to carwash wastewaters for reuse. Part 1: anodic oxidation with diamond and lead dioxide anodes. J Electroanal Chem 638: 28–32

Panizza M, Bocca C, Cerisola G (2000) Electrochemical treatment of wastewater containing polyaromatic organic pollutants. Water Res 34(9):2601–2605

Papastefanakis N, Mantzavinos D, Katsaounis A (2010) DSA electrochemical treatment of olive mill wastewater on Ti/RuO_2 anode. J Appl Electrochem 40:729–737

Pavlov D (1992) The lead-acid battery lead dioxide active mass: a gel-crystal system with proton and electron conductivity. J Electrochem Soc 139:3075–3080

Perednis D, Gauckler LJ (2005) Thin film deposition using spray pyrolysis. J Electroceram 14:103–111

Radjenovic J, Escher BI, Rabaey K (2011) Electrochemical degradation of the β-blocker metoprolol by Ti/$Ru_{0.7}Ir_{0.3}O_2$ and Ti/SnO_2-Sb electrodes. Water Res 45:3205–3214

Riihelä D, Ritala M, Matero R, Leskelä M (1996) Electronics, optics and opto-electronics, introducing atomic layer epitaxy for the deposition of optical thin films. Thin Solid Films 289:250–255

Rodgers JD, Jedral W, Bunce NJ (1999) Electrochemical oxidation of chlorinated phenols. Environ Sci Technol 33:1453–1457

Rosales E, Pazos M, Longo MA, Sanromán MA (2009) Influence of operational parameters on electro-Fenton degradation of organic pollutants from soil. J Enviro Sci Health Part A: Toxic/Hazard Subst Environ Eng 44:1104–1110

Sakalis A, Vanĕrková D, Holčapek M, Jandera P, Voulgaropoulos A (2007) Electrochemical treatment of a simple azodye and analysis of the degradation products using high performance liquid chromatography-diode array detection-tandem mass spectrometry. Chemosphere 67:1940–1948

Sala M, Gutiérrez-Bouzán MC (2012) Electrochemical techniques in textile processes and wastewater treatment. Int J Photoenergy 2012:1–12

Scialdone O (2009) Electrochemical oxidation of organic pollutants in water at metal oxide electrodes: a simple theoretical model including direct and indirect oxidation processes at the anodic surface. Electrochim Acta 54:6140–6147

Scialdone O, Randazzo S, Galia A, Filardo G (2009a) Electrochemical oxidation of organics at metal oxide electrodes: the incineration of oxalic acid at IrO_2–Ta_2O_5 (DSA-O_2) anode. Electrochim Acta 54: 1210–1217

Scialdone O, Randazzo S, Galia A, Silvestri G (2009b) Electrochemical oxidation of organics in water: role of operative parameters in the absence and in the presence of NaCl. Water Res 43:2260–2272

Simond O, Schaller V, Comninellis C (1997a) Theoretical model for the anodic oxidation of organics on metal oxide electrodes. Electrochim Acta 42(13–14):2009–2012

Simond O, Schaller V, Comninellis C (1997b) Anodic oxidation of organics on Ti/IrO_2 anodes using Nafion® as electrolyte. Electrochim Acta 42(13–14):2013–2018

Soloman PA, Basha CA, Velan M, Ramamurthi V, Koteeswaran K, Balasubramanian N (2009) Electrochemical degradation of remazol Black B dye effluent. Clean 37(11):8–900

Song S, Zhan L, He Z, Lina L, Tu J, Zhang Z, Chen J, Xu L (2010a) Mechanism of the anodic oxidation of 4-chloro-3-methyl phenol in aqueous solution using Ti/SnO_2–Sb/PbO_2 electrodes. J Hazard Mater 175:614–621

Song S, Fan J, He Z, Zhan L, Liu Z, Chen J, Xu X (2010b) Electrochemical degradation of azo dye C.I. Reactive Red 195 by anodic oxidation on Ti/SnO_2–Sb/PbO_2 electrodes. Electrochim Acta 55:3606–3613

Soni BD, Ruparelia JP (2012) Studies on effects of electrodes for decontamination of dyes from wastewater. J Environ Res Dev 6:973–979

Trasatti S (2000) Electrocatalysis: understanding the success of DSR®. Electrochim Acta 45:2377–2385

Vicent F, Morallón E, Quijada C, Vâzquez JL, Aldaz A, Cases F (1998) Characterization and stability of doped SnO_2 anodes. J Appl Electrochem 28:607–612

Wang YH, Chan KY, Li XY (2006) Electrochemical degradation of 4-chlorophenol at nickel-antimony doped tin oxide electrode. Chemosphere 65:1087–1093

Wang YQ, Gu B, Xu WL (2009) Electro-catalytic degradation of phenol on several metal-oxide anodes. J Hazard Mater 162:1159–1164

Wang KS, Wei MC, Peng TH, Li HC, Chao SJ, Hsu TF, Lee HS, Chang SH (2010a) Treatment and toxicity evaluation of methylene blue using electrochemical oxidation, fly ash adsorption and combined electrochemical oxidation-fly ash adsorption. J Environ Manage 91: 1778–1784

Wang Y, Shen Z, Li Y, Niu J (2010b) Electrochemical properties of the erbium–chitosan–fluorine-modified PbO_2 electrode for the degradation of 2,4-dichlorophenol in aqueous solution. Chemosphere 79: 987–996

Watts RJ, Wyeth MS, Finn DD, Teel AL (2008) Optimization of Ti/SnO_2–Sb_2O_5 anode preparation for electrochemical oxidation of organic contaminants in water and wastewater. J Appl Electrochem 38:31–37

Xu H, Li AP, Qi Q, Jiang W, Sun YM (2012) Electrochemical degradation of phenol on the La and Ru doped Ti/SnO_2-Sb electrodes. Korean J Chem Eng 29:1178–1186

Yang X, Zou R, Huo F, Cai D, Xiao D (2009) Preparation and characterization of Ti/SnO_2–Sb_2O_3–Nb_2O_5/PbO_2 thin film as electrode material for the degradation of phenol. J Hazard Mater 164:367–373

Yeo IH, Wen S, Mho SI (2010) Effect of interfacial oxides on the electrochemical activity of lead dioxide film electrodes on a Ti substrate. Ananl Sci 26:39–44

Yusta FJ, Hitchman ML, Shamlian SH (1997) CVD preparation and characterization of tin dioxide films for electrochemical applications. J Mater Chem 7(8):1421–1427

Zaviska F, Drogui P, Blais JF, Mercier G (2009) In situ active chlorine generation for the treatment of dye-containing effluents. J Appl Electrochem 39:2397–2408

Zhao WR, Xu XH, Shi HX, Wang DH (2003) Degradation mechanism of cationic red X-GRL by ozonation. Chin Chem Lett 14:1309–1312

Zhoua M, He J (2008) Degradation of cationic red X-GRL by electrochemical oxidation on modified PbO_2 electrode. J Hazard Mater 153:357–363

Zhuo Q, Deng S, Yang B, Huang J, Yu G (2011) Efficient electrochemical oxidation of perfluorooctanoate using a Ti/SnO_2-Sb-Bi anode. Environ Sci Technol 45:2973–2979